

# Quantum spin representation for the Navier-Stokes equation

Zhaoyuan Meng<sup>1</sup> and Yue Yang<sup>1,2,\*</sup>

<sup>1</sup>*State Key Laboratory for Turbulence and Complex Systems,  
College of Engineering, Peking University, Beijing 100871, PR China*

<sup>2</sup>*HEDPS-CAPT, Peking University, Beijing 100871, PR China*  
(Dated: March 4, 2024)

We develop a quantum representation for Newtonian viscous fluid flows by establishing a mapping between the Navier-Stokes equation (NSE) and the Schrödinger-Pauli equation (SPE). The proposed nonlinear SPE incorporates the two-component wave function and the imaginary diffusion. Consequently, classical fluid flow can be interpreted as a non-Hermitian quantum spin system. Using the SPE-based numerical simulation of viscous flows, we demonstrate the quantum/wave-like behavior in flow dynamics. Furthermore, the SPE equivalent to the NSE can facilitate the quantum simulation of fluid dynamics.

*Introduction.*— Fluid dynamics and quantum mechanics represent physics at macroscopic and microscopic scales, respectively, but they can demonstrate remarkable similarities. Some macroscopic flows exhibit quantum phenomena, such as the wave-particle duality exhibited by walking droplets [1–3], the Casimir effect observed in turbulence and turbulent plasmas [4–6], and the Saffman-Taylor fingering akin to the growth of an electronic droplet in the quantum Hall regime [7]. Conversely, quantum spin systems can display emergent hydrodynamic behavior [8, 9]. The Schrödinger-like quantum representation has proven useful in capturing certain flow phenomena, including superfluids [10, 11], quantum plasmas [12], non-Abelian fluids [13], soliton dynamics of vortex filaments [14], and topological active matter [15].

In mathematics, fluid dynamics and quantum mechanics are described by two seemingly distinct equations, the Navier-Stokes equation (NSE) and the Schrödinger equation, respectively. Despite their apparent differences, some attempts have been made to establish an explicit mathematical connection between the two fields. Madelung [16] recast the Schrödinger equation into a modified Euler equation for compressible potential flows, but this transform has little application due to the lack of the vorticity, a key component in shear flows and turbulence.

Several works have striven to incorporate the finite vorticity and viscous effects into the quantum representation of fluid dynamics. Sorokin [17] extended the Madelung transform to account for finite vorticity using the two-component wave function. Chern *et al.* [18, 19] employed the two-component wave function to characterize the incompressible Schrödinger flow with an artificial body force. Meng and Yang [20] generalized the incompressible Schrödinger flow to compressible flows. Salasnich *et al.* [21] introduced the imaginary diffusion of the wave function to achieve the correct dissipation for Newtonian fluids, but they only examined the single-component wave function for potential flows.

Here we develop a comprehensive quantum representation for real fluid flows by establishing an explicit mapping between the NSE and the Schrödinger-Pauli equation (SPE) with the two-component wave function. The proposed nonlinear SPE for a quantum spin system is a Hamiltonian formulation [22] for both compressible and incompressible viscous flow with finite vorticity. The imaginary diffusion [21] is incorporated into the SPE, leading to a non-Hermitian quantum system.

The classical Madelung transform [16] is related to the de Broglie-Bohm interpretation of quantum mechanics [23–27]. Conversely, the present NSE-SPE mapping can facilitate quantum computing of fluid dynamics through Hamiltonian simulation [20, 28]. The quantum simulation [29] of fluid flows (as a unique quantum spin system) holds immense potential in various applications, e.g., in aerospace engineering and weather forecasting [30–32].

*Schrödinger-Pauli formulation of the NSE.*— We employ the hydrodynamic formulation of the SPE [20] to represent the compressible/incompressible NSE with finite vorticity, highlighting the essential role of the vorticity  $\boldsymbol{\omega} \equiv \nabla \times \mathbf{u}$  in viscous flows [33], with the velocity  $\mathbf{u}$ . The quantum system governed by the SPE is characterized by a two-component spinor wave function  $|\psi_{\pm}\rangle \equiv [|\psi_{+}\rangle, |\psi_{-}\rangle]^T$ , where  $|\psi_{+}\rangle$  and  $|\psi_{-}\rangle$  are the spin-up and -down components, respectively [34–36]. The probability current is given by  $\mathbf{J} \equiv (\hbar/m)\langle \nabla \psi_{\pm}, i\psi_{\pm} \rangle_{\mathbb{R}}$ , with the Planck constant  $\hbar$ , particle mass  $m$ , and operator  $\langle \phi, \psi \rangle_{\mathbb{R}} \equiv \sum_{i=1}^2 (x_i \alpha_i + y_i \beta_i)$ ,  $\forall \phi = [x_1 + iy_1, x_2 + iy_2]^T$  and  $\psi = [\alpha_1 + i\beta_1, \alpha_2 + i\beta_2]^T$ . The flow velocity is then defined as

$$\mathbf{u} \equiv \frac{\mathbf{J}}{\rho} = \frac{\hbar}{m} \frac{\langle \nabla \psi_{\pm}, i\psi_{\pm} \rangle_{\mathbb{R}}}{\langle \psi_{\pm}, \psi_{\pm} \rangle_{\mathbb{R}}} \quad (1)$$

via the generalized Madelung transform [20], where

$$\rho \equiv \langle \psi_{\pm}, \psi_{\pm} \rangle_{\mathbb{R}} = |\psi_{+}|^2 + |\psi_{-}|^2 \quad (2)$$

is the fluid density.

\* yyg@pku.edu.cn

We recast the compressible (i.e., general) NSE

$$\begin{cases} \frac{\partial \rho}{\partial t} + \nabla \cdot (\rho \mathbf{u}) = 0, \\ \frac{\partial \mathbf{u}}{\partial t} + \mathbf{u} \cdot \nabla \mathbf{u} = -\frac{1}{\rho} \nabla p + \frac{\mu}{3\rho} \nabla (\nabla \cdot \mathbf{u}) + \frac{\mu}{\rho} \Delta \mathbf{u} \end{cases} \quad (3)$$

into a nonlinear SPE

$$\begin{aligned} i\hbar \frac{\partial}{\partial t} |\psi_{\pm}\rangle = & \left[ \left( 1 - i \frac{2m\mu}{\hbar\rho} \right) \frac{\hat{\mathbf{p}}^2}{2m} + \tilde{p} + \frac{\hbar^2}{2m\rho} |\nabla \psi_{\pm}|^2 \right. \\ & \left. + i \frac{\hbar\mu}{2} \frac{2|\nabla \psi_{\pm}|^2 - \Delta\rho}{\rho^2} \right] \mathbf{I} |\psi_{\pm}\rangle + \boldsymbol{\sigma} \cdot \mathbf{B} |\psi_{\pm}\rangle. \end{aligned} \quad (4)$$

The derivation for this hydrodynamic SPE is detailed in the Supplementary Material (SM) [37]. Here,  $\hat{\mathbf{p}} = -i\hbar\nabla$  is the momentum operator in the position representation,  $\mu$  is a constant viscosity coefficient,  $\tilde{p} = P - m|\mathbf{u}|^2/2 + \hbar\mathbf{s} \cdot \mathbf{f}/\rho$  is a modified pressure with  $P = \int m/\rho d [p - \hbar^2|\nabla\rho|^2/(4m^2\rho) - \mu\nabla \cdot \mathbf{u}/3]$ , the static pressure  $p$  given by the equation of state, and a vector  $\mathbf{f} \in \mathbb{R}^3$  to be determined,  $\mathbf{I}$  is the  $2 \times 2$  identity matrix,  $\boldsymbol{\sigma}$  is the Pauli vector,  $\mathbf{B} = \mathbf{T}_0 \cdot \hat{\mathbf{B}}$  is a spin-coupled vector given by  $\hat{\mathbf{B}} = \hbar^2 \Delta \mathbf{s} / (4m\rho) - \hbar \mathbf{f}$  and an anti-diagonal matrix  $\mathbf{T}_0$  with elements  $T_{0,ij} = (-1)^{i-1} \delta_{j,4-i}$ ,  $i, j = 1, 2, 3$ , and

$$\mathbf{s} \equiv (|\psi_+|^2 - |\psi_-|^2, i(\psi_+^* \psi_- - \psi_+ \psi_-^*), \psi_+^* \psi_- + \psi_+ \psi_-^*) \quad (5)$$

is the spin vector; the superscript “\*” denotes the complex conjugate, and the matrix  $\mathbf{T}_0$  the reflection of the  $y$ -axis in  $\mathbb{R}^3$  preserving chirality. Note that Eq. (4) is closed with the equations of state and energy in general, and when  $p$  is solely determined by  $\psi_{\pm}$  in particular, such as in the quantum potential [26, 27].

We employ the Moore-Penrose solution for  $\mathbf{f}$  as

$$[f_1 \ f_2 \ f_3]^T = \mathbf{A}^T (\mathbf{A} \mathbf{A}^T)^{-1} [\mathcal{S}_x \ \mathcal{S}_y \ \mathcal{S}_z]^T, \quad (6)$$

which avoids the singularity of  $|\mathbf{A}| = 0$  and minimizes  $\|\mathbf{f}\|_2$ , with matrix elements  $A_{ij} = \partial_i s_j - s_j \partial_i \ln \rho$  and

$$\begin{aligned} \mathcal{S} = & \frac{\hbar}{4m\rho^2} \nabla \rho \cdot \left[ \nabla (\rho \nabla \rho) - \nabla \nabla \mathbf{s} \cdot \mathbf{s} + \frac{8m^2\mu}{\hbar^2} \rho \nabla \mathbf{u} \right] \\ & + \frac{2m\mu}{\hbar\rho} |\nabla \psi_{\pm}|^2 \mathbf{u} - \frac{m\mu}{\hbar} (\nabla \cdot \mathbf{u} + \mathbf{u} \cdot \nabla \ln \rho) \nabla \ln \rho. \end{aligned}$$

The energy expectation of the quantum system in Eq. (4) is

$$\begin{aligned} \langle E \rangle = & \int_{\mathcal{D}} \left[ \frac{m\rho|\mathbf{u}|^2}{2} + \rho P + \frac{\hbar^2}{4m} \left( \Delta\rho + \frac{|\nabla\rho|^2}{\rho} \right) \right] dx \\ & + i\hbar\mu \int_{\mathcal{D}} \mathbf{u} \cdot \nabla \ln \rho dx \end{aligned} \quad (7)$$

in the solution domain  $\mathcal{D}$ . Hence, the Hamiltonian of Eq. (4) is non-Hermitian for  $\mu \neq 0$ , as  $\langle E \rangle$  is complex-valued. The real part of  $\langle E \rangle$  comprises the total kinetic energy, the pressure energy, and the compressible effect.

For the inviscid flow with  $\mu = 0$ , Eq. (3) degenerates to the compressible Euler equation (see SM [37]).

A particular case of Eq. (3) is for the incompressible flow with constant density  $\rho = \rho_0$ . Here,  $|\psi_{\pm}\rangle$  resembling the momentum eigenstate (i.e., the plane wave) is subjected to a solenoidal constraint  $\langle \Delta \psi_{\pm}, i\psi_{\pm} \rangle_{\mathbb{R}} = 0$  for the divergence-free velocity. The incompressible NSE

$$\begin{cases} \nabla \cdot \mathbf{u} = 0, \\ \frac{\partial \mathbf{u}}{\partial t} + \mathbf{u} \cdot \nabla \mathbf{u} = -\nabla \frac{p}{\rho_0} + \nu \Delta \mathbf{u} \end{cases} \quad (8)$$

with constant kinematic viscosity  $\nu \equiv \mu/\rho_0$  is reformulated into a nonlinear SPE

$$\begin{aligned} i\hbar \frac{\partial}{\partial t} |\psi_{\pm}\rangle = & \left[ \left( 1 - i \frac{2m\nu}{\hbar} \right) \frac{\hat{\mathbf{p}}^2}{2m} + \tilde{p} + \frac{\hbar^2}{2m\rho_0} |\nabla \psi_{\pm}|^2 \right. \\ & \left. + i \frac{\hbar\nu}{\rho_0} |\nabla \psi_{\pm}|^2 \right] \mathbf{I} |\psi_{\pm}\rangle + \boldsymbol{\sigma} \cdot \mathbf{B} |\psi_{\pm}\rangle, \end{aligned} \quad (9)$$

with a modified pressure  $\tilde{p} = m(p/\rho_0 - |\mathbf{u}|^2/2 - \phi_h) + \hbar\mathbf{s} \cdot \mathbf{f}/\rho_0$ .

Here,  $\mathbf{f}$  is given by Eq. (6) with  $A_{ij} = \partial_i s_j$  and  $\mathcal{S} = 2m\nu |\nabla \psi_{\pm}|^2 \mathbf{u}/\hbar + m\rho_0 \nabla \phi_h/\hbar$ , and the topology-related scalar  $\phi_h$  satisfies

$$\boldsymbol{\omega} \cdot \nabla \phi_h = -\frac{2\nu}{\rho_0} |\nabla \psi_{\pm}|^2 h \quad (10)$$

with the helicity density  $h \equiv \mathbf{u} \cdot \boldsymbol{\omega}$ . Local solutions of  $\phi_h$  to Eq. (10) can exist [38], but the existence and uniqueness of global solutions to Eq. (10) are not guaranteed [39, 40], except that  $\mathbf{f}$  can be obtained by setting  $\phi_h = 0$  for simple flows with  $h = 0$ . For  $\nu = 0$ , Eq. (8) is reduced to the incompressible Euler equation [41], and the corresponding SPE in Eq. (9) is accordingly simplified with  $\mathbf{f} = \mathbf{0}$ .

The NSE-SPE mapping for incompressible flows exhibits a remarkable geometric relation. It transforms the vorticity in  $\mathbb{R}^3$  into a spin vector in  $\mathbb{S}^2$ , thereby associating each vortex line in 3D space with a point on the Bloch sphere [19, 20, 41].

The lengthy derivation for SPEs in Eqs. (4) and (9) (see SM [37]) is outlined below. It begins from the hydrodynamic Schrödinger equation [18–20] for a non-Newtonian fluid flow. The present SPE adds the imaginary diffusion of the wave function [21] and three terms to be determined, including the real potential that applies a pressure to the fluid, the imaginary potential that balances the imaginary diffusion to ensure the particle-number conservation, and the Stern-Gerlach term  $\boldsymbol{\sigma} \cdot \mathbf{B}$  that cancels the artificial body forces (e.g. the Landau-Lifshitz force [20]) in the momentum equation. These undetermined terms are derived by substituting the proposed SPE into the continuity and momentum fluid equations with Eqs. (1) and (2).

*Hamiltonian of the hydrodynamic SPE*— The general form  $i\hbar\partial_t |\psi_{\pm}\rangle = \hat{H} |\psi_{\pm}\rangle$  of the SPE for fluid flows has

the Hamiltonian

$$\hat{H} = \left[ \frac{\hat{\mathbf{p}}^2}{2m} + V_r + i \left( \frac{\hat{\mathbf{p}}^2}{2m_i} + V_i \right) \right] \mathbf{I} + \boldsymbol{\sigma} \cdot \mathbf{B}. \quad (11)$$

It depends on the particle mass  $m$ , virtual mass  $m_i$ , real potential  $V_r$ , imaginary potential  $V_i$ , and the spin-coupled vector  $\mathbf{B}$ . Note that the present SPE does not involve an external electromagnetic field in the standard SPE [42].

Table I presents the expressions of  $\hat{H}$  for various flows. The introduction of the viscous dissipation of Newtonian fluids requires adding the imaginary diffusion [21] of  $\psi_{\pm}$  with a virtual mass  $m_i$ , which makes the quantum system non-Hermitian. To ensure the probability conservation, we invoke the imaginary potential  $V_i$ . Hence, despite the non-Hermiticity of the Hamiltonian in the viscous flow, the quantum state evolves unitarily, enabling its potential implementation on a gate-based quantum computer.

The anti-Hermitian term  $i\hat{H}_D$  [15, 43], with  $\hat{H}_D = \hat{H}_D^\dagger$  and  $\hat{H}_D = \hat{\mathbf{p}}^2/(2m_i) + V_i$ , arises from the viscous dissipation in fluids. The virtual mass, proportional to  $1/\nu$ , has  $m_i \rightarrow \infty$  in the inviscid flow without the non-Hermitian effect.

*Quantum representation for flow evolution.*— We illustrate the quantum/wave-like behavior in the flow evolution using the SPE-based numerical simulation for a 1D compressible flow and a 2D incompressible Taylor-Green (TG) flow [44]. Without loss of generality, we set  $\rho_0 = 1$ ,  $\hbar = 1$ , and  $m = 1$ . We develop a numerical method to solve the nonlinear SPE in Eqs. (4) and (9) with periodic boundary conditions. The fraction-step Fourier method based on the second-order Trotter decomposition is employed for time integration. The algorithm is detailed in SM [37]. For brevity, the normalization constant of the wave function is omitted in the numerical simulation, such that  $\langle \psi_{\pm} | \psi_{\pm} \rangle \neq 1$ .

First, we consider a 1D compressible flow governed by the Burgers equation at  $x \in [0, 2\pi]$  with the initial condition  $u(x, 0) = \sin x$ , boundary condition  $u(0, t) = u(2\pi, t) = 0$ , and  $\nu = 0.01$ . The initial wave function is  $\psi_+(x, 0) = \cos x e^{-i \cos x}$  and  $\psi_-(x, 0) = \sin x e^{-i \cos x}$ .

This flow is a simplified model for the formation of a shock wave. In Fig. 1(a), the reconstructed velocity from the numerical solution to Eq. (1) agrees with the exact solution. The fluids on both sides converge to the center at  $x = \pi$ , forming a shock. Note that the numerical solution is only shown at  $t \leq 1$ , due to strong numerical oscillations in solving the SPE at later times. In Fig. 1(b), the probability of particle occurrence accumulates near the shock. Thus, the velocity discontinuity corresponds to the maximum probability amplitude in the wave-function representation.

The quantum representation can shed light on the flow evolution. Figures 1(c) and (d) plot the phases  $\phi_{\pm} \equiv \arg(\psi_{\pm})$  of spin-up and -down components, respectively. The contour of  $\phi_+$  exhibits two lines separating large and near-zero values, indicating two converging waves with

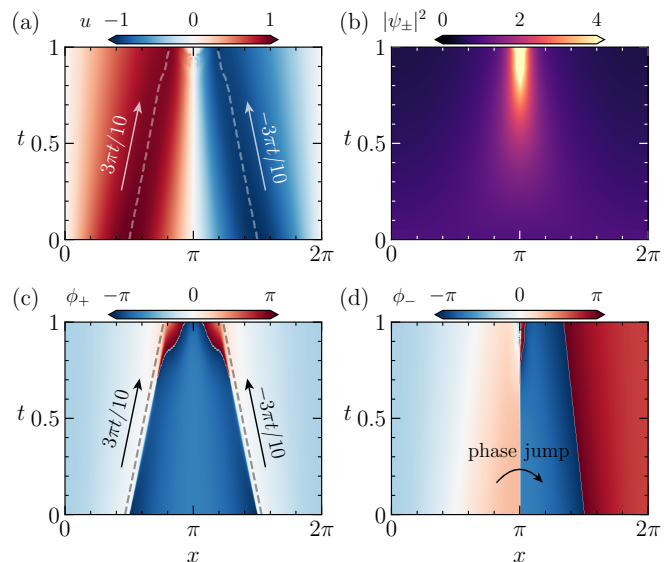


FIG. 1. Numerical solutions to the SPE for the Burgers equation: (a) velocity reconstructed from Eq. (1), (b) particle's probability density, and (c, d) phases of spin-up and -down components.

the speed of  $\pm 3\pi/10$ . They coincide with the maximum-speed locations (dashed lines in Fig. 1(a) and (c)), and defining the shock emergence at  $t = 5/3$ . Furthermore, the phase jump  $\phi_-(\pi^-, t) - \phi_-(\pi^+, t) = \pi$  at the initial time in Fig. 1(d) signals the shock location  $x = \pi$  at later times. Some supplementary data is provided in SM [37].

Second, we consider the 2D incompressible TG viscous flow in a periodic box  $\mathbf{x} \in [0, 2\pi]^2$  with  $\mathbf{u}(\mathbf{x}, 0) = \sin x \cos y \mathbf{e}_x - \cos x \sin y \mathbf{e}_y$  and  $\nu = 1$ , where  $\{\mathbf{e}_x, \mathbf{e}_y\}$  are the Cartesian unit vectors. The initial wave function is  $\psi_+(\mathbf{x}, 0) = \cos[H(x)]e^{i \cos y(2 - \cos x)}$  and  $\psi_-(\mathbf{x}, 0) = \sin[H(x)]e^{-i \cos y(2 + \cos x)}$ , with  $H(x) = x/2$  for  $0 \leq x \leq \pi$  and  $H(x) = \pi - x/2$  for  $\pi < x \leq 2\pi$ .

This flow illustrates the quantum representation for the viscous effect. The exponential decay of the velocity and vorticity is observed in Fig. 2(a), consistent with the exact solution. The isolines of the real (solid red lines) and imaginary (dashed blue lines) parts of  $\psi_+$  at  $t = 0, 0.5$ , and 1 are plotted Fig. 2(b). They are interlaced at the initial time, and then elongate along the  $x$ - and  $y$ -directions in the viscous decaying process. In the pilot wave theory [23–27], the smoothing of  $\psi_{\pm}$  reduces the velocity of fluid particles, consistent with the observed attenuation of vortex rotation in Fig. 2(a). The particle probability distribution in the momentum space converges to the zero state in Fig. 2(c), implying that the fluid velocity decays to zero under viscous dissipation. Some supplementary data is provided in SM [37].

*Discussion.*— We develop a quantum representation for Navier-Stokes fluid dynamics, establishing a mapping between the hydrodynamic SPE in Eqs. (4) and (9) and the compressible and incompressible NSEs. Beyond the classical Madelung transform [16], the present SPE de-

TABLE I. Summary of the Hermiticity of the Hamiltonian, virtual mass  $m_i$ , real potential  $V_r$ , imaginary potential  $V_i$ , and spin-coupled vector  $\tilde{\mathbf{B}}$  in Eq. (11) for different flow equations.

Equation	Hamiltonian	$m_i$	$V_r$	$V_i$	$\tilde{\mathbf{B}} = \mathbf{T}_0 \cdot \mathbf{B}$
Compressible Navier-Stokes equation	non-Hermitian	$-\frac{\hbar\rho}{2\mu}$	$\tilde{p} + \frac{\hbar^2}{2m\rho}  \nabla\psi_{\pm} ^2$	$\frac{\hbar\mu}{2} \frac{2 \nabla\psi_{\pm} ^2 - \Delta\rho}{\rho^2}$	$\frac{\hbar^2}{4m\rho} \Delta\mathbf{s} - \hbar\mathbf{f}$
Incompressible Navier-Stokes equation	non-Hermitian	$-\frac{\hbar}{2\nu}$	$\tilde{p} + \frac{\hbar^2}{2m\rho_0}  \nabla\psi_{\pm} ^2$	$\frac{\hbar\nu}{\rho_0}  \nabla\psi_{\pm} ^2$	$\frac{\hbar^2}{4m\rho_0} \Delta\mathbf{s} - \hbar\mathbf{f}$
Compressible Euler equation	Hermitian	$\infty$	$\tilde{p} + \frac{\hbar^2}{2m\rho}  \nabla\psi_{\pm} ^2$	0	$\frac{\hbar^2}{4m\rho} \Delta\mathbf{s} - \hbar\mathbf{f}$
Incompressible Euler equation [41]	Hermitian	$\infty$	$\tilde{p} + \frac{\hbar^2}{2m\rho_0}  \nabla\psi_{\pm} ^2$	0	$\frac{\hbar^2}{4m\rho_0} \Delta\mathbf{s}$

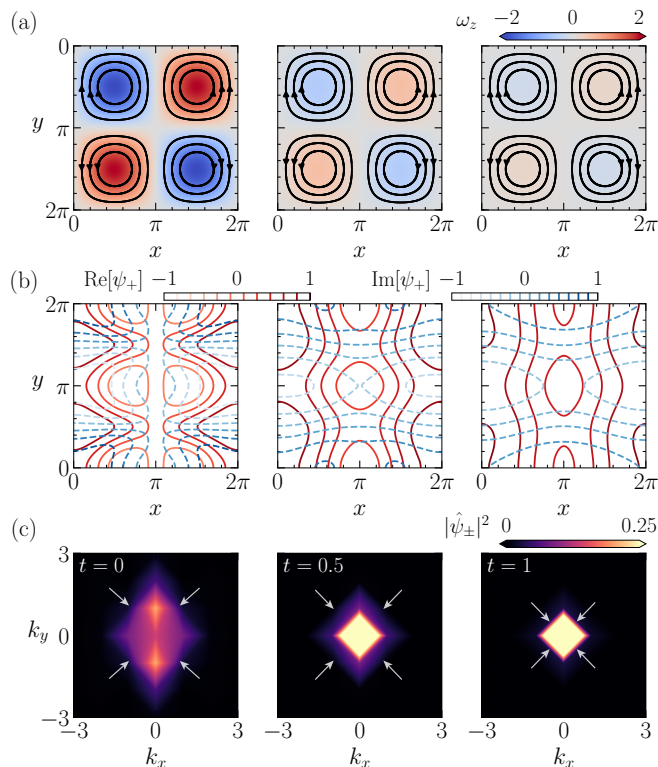


FIG. 2. Numerical results obtained from the simulation of Eq. (9) for the 2D TG flow at  $t = 0$  (left),  $0.5$  (middle), and  $1$  (right). (a) Streamlines and vorticity contour. (b) Contours of the real (solid red curves) and imaginary (dashed blue curves) parts of the spin-up component. (c) Particle probability distribution in the momentum space.

scribes a quantum spin system with a two-component spinor wave function, corresponding to a flow with finite vorticity. The wave function undergoes imaginary diffusion [21] to account for the viscous dissipation of Newtonian fluids, rendering the quantum system non-Hermitian. To preserve probability conservation, an imaginary potential is introduced.

On the other hand, a globally smooth wave function may not exist for a velocity field with vorticity nulls or unclosed vortex lines [41]. Therefore, the SPE is limited

to the NSE with a subset of initial conditions. A useful approximation of the wave function can be obtained for a given velocity field using the numerical optimization [19].

We demonstrate the quantum/wave-like behavior of the flow evolution for a 1D compressible flow and a 2D incompressible TG flow using the SPE-based numerical simulation. In the compressible flow, the wave-function representation exhibits a maximum particle probability at the velocity discontinuity near the shock, and the initial phase jump signals the location of shock formation at later times. In the incompressible flow, the real and imaginary parts of the wave function are initially interlaced, and then elongate along the  $x$ - and  $y$ -directions as the flow undergoes viscous dissipation. The particle probability distribution in the momentum space approaches the zero state, reflecting the quantum representation of viscous effects.

The present study can open new research avenues in the interdisciplinary study of fluid dynamics and quantum mechanics. First, we demonstrate the potential of quantum simulation [29] for classical fluid dynamics, including viscous and vortical flows. The SPE, a Hamiltonian system, is more tractable than the NSE for quantum computing [20]. The synergy of computational fluid dynamics and quantum computing heralds the next-generation simulation method [30–32].

However, there are two primary obstacles that need to be addressed – the nonlinearity and the non-Hermitian Hamiltonian in the SPE. The former can be partially resolved by the mean-field linearization [45], which converts the nonlinear potential on a single particle into a linear interaction term in a quantum many-body system. For the latter, since the quantum state evolution maintains unitary and the non-Hermitian part is anti-Hermitian [43], it seems feasible to implement this Hamiltonian on a gate-based quantum computer.

Second, the hydrodynamic SPE enables studying classical turbulence as a quantum system, thereby extending previous research on quantum turbulence [46, 47]. This approach offers a unique perspective, leveraging the inherent Lagrangian nature of the quantum representation to facilitate the investigation of vortex-surface evolution in incompressible flows [41, 48]. Furthermore, the NSE-

SPE correspondence may unveil novel quantum effects on classical mechanical systems within the framework of non-Hermitian physics [43, 49, 50].

This work has been supported by the National Natural Science Foundation of China (Grant Nos. 11925201 and 11988102), the National Key R&D Program of China (Grant Nos. 2023YFB4502600 and 2020YFE0204200), and the Xplore Prize.

- 
- [1] T. Gilet and J. W. M. Bush, Chaotic bouncing of a droplet on a soap film, *Phys. Rev. Lett.* **102**, 014501 (2009).
- [2] J. W. M. Bush and A. U. Oza, Hydrodynamic quantum analogs, *Rep. Prog. Phys.* **84**, 017001 (2020).
- [3] P. J. Sáenz, G. Pucci, S. E. Turton, A. Goujon, R. R. Rosales, J. Dunkel, and J. W. M. Bush, Emergent order in hydrodynamic spin lattices, *Nature* **596**, 58 (2021).
- [4] M. Kardar and R. Golestanian, The “friction” of vacuum, and other fluctuation-induced forces, *Rev. Mod. Phys.* **71**, 1233 (1999).
- [5] M. Davoodianidalik, H. Punzmann, H. Kellay, H. Xia, M. Shats, and N. Francois, Fluctuation-induced interaction in turbulent flows, *Phys. Rev. Lett.* **128**, 024503 (2022).
- [6] J. T. Mendonça, R. Bingham, P. K. Shukla, and D. Resendes, Casimir effect in a turbulent plasma, *Phys. Lett. A* **289**, 233 (2001).
- [7] O. Agam, E. Bettelheim, P. Wiegmann, and A. Zabrodin, Viscous fingering and the shape of an electronic droplet in the quantum Hall regime, *Phys. Rev. Lett.* **88**, 236801 (2002).
- [8] C. Zu, F. Machado, B. Ye, S. Choi, B. Kobrin, T. Mittiga, S. Hsieh, P. Bhattacharyya, M. Markham, D. Twitchen, *et al.*, Emergent hydrodynamics in a strongly interacting dipolar spin ensemble, *Nature* **597**, 45 (2021).
- [9] M. K. Joshi, F. Kranzl, A. Schuckert, I. Lovas, C. Maier, R. Blatt, M. Knap, and C. F. Roos, Observing emergent hydrodynamics in a long-range quantum magnet, *Science* **376**, 720 (2022).
- [10] E. P. Gross, Structure of a quantized vortex in boson systems, *Il Nuovo Cimento* **20**, 454 (1961).
- [11] L. P. Pitaevskii, Vortex lines in an imperfect Bose gas, *Sov. Phys. JETP*. **13**, 451 (1961).
- [12] M. Marklund and G. Brodin, Dynamics of spin-1/2 quantum plasmas, *Phys. Rev. Lett.* **98**, 025001 (2007).
- [13] P. J. Love and B. M. Boghosian, Quaternionic Madelung transformation and non-Abelian fluid dynamics, *Physica A* **332**, 47 (2004).
- [14] H. Hasimoto, A soliton on a vortex filament, *J. Fluid Mech.* **51**, 477 (1972).
- [15] K. Sone and Y. Ashida, Anomalous topological active matter, *Phys. Rev. Lett.* **123**, 205502 (2019).
- [16] E. Madelung, Quantentheorie in hydrodynamischer form, *Z. Phys.* **40**, 322 (1927).
- [17] A. L. Sorokin, Madelung transformation for vortex flows of a perfect liquid, *Dokl. Phys.* **46**, 576 (2001).
- [18] A. Chern, F. Knöppel, U. Pinkall, P. Schröder, and S. Weißmann, Schrödinger’s smoke, *ACM Trans. Graph.* **35**, 1 (2016).
- [19] A. Chern, F. Knöppel, U. Pinkall, and P. Schröder, Inside fluids: Clebsch maps for visualization and processing, *ACM Trans. Graph.* **36**, 1 (2017).
- [20] Z. Meng and Y. Yang, Quantum computing of fluid dynamics using the hydrodynamic Schrödinger equation, *Phys. Rev. Res.* **5**, 033182 (2023).
- [21] L. Salasnich, S. Succi, and A. Tiribocchi, Quantum wave representation of dissipative fluids (2023), arXiv:2308.05879.
- [22] P. J. Morrison, Hamiltonian description of the ideal fluid, *Rev. Mod. Phys.* **70**, 467 (1998).
- [23] D. Bohm, A Suggested Interpretation of the Quantum Theory in Terms of “Hidden” Variables. I, *Phys. Rev.* **85**, 166 (1952).
- [24] T. Takabayasi, On the formulation of quantum mechanics associated with classical pictures, *Prog. Theor. Phys.* **8**, 143 (1952).
- [25] T. Takabayasi, Remarks on the Formulation of Quantum Mechanics with Classical Pictures and on Relations between Linear Scalar Fields and Hydrodynamical Fields, *Prog. Theor. Phys.* **9**, 187 (1953).
- [26] R. E. Wyatt, *Quantum Dynamics with Trajectories – Introduction to Quantum Hydrodynamics*, Vol. 28 (Springer, 2005).
- [27] D. Bohm, *Quantum Theory* (Courier Corporation, 2012).
- [28] Z. Lu and Y. Yang, Quantum computing of reacting flows via Hamiltonian simulation (2023), arXiv:2312.07893.
- [29] R. P. Feynman, Simulating physics with computers, *Int. J. Theor. Phys.* **21**, 467 (1982).
- [30] P. Givi, A. J. Daley, D. Mavriplis, and M. Malik, Quantum speedup for aerospace and engineering, *AIAA J.* **58**, 8 (2020).
- [31] S. Succi, W. Itani, K. Sreenivasan, and R. Steijl, Quantum computing for fluids: Where do we stand?, *Europhys. Lett.* **144**, 10001 (2023).
- [32] S. S. Bharadwaj and K. R. Sreenivasan, Hybrid quantum algorithms for flow problems, *Proc. Natl. Acad. Sci. U.S.A.* **120**, e2311014120 (2023).
- [33] P. G. Saffman, *Vortex Dynamics*, Cambridge Monographs on Mechanics (Cambridge University Press, 1993).
- [34] E. J. Mueller and T.-L. Ho, Two-component Bose-Einstein condensates with a large number of vortices, *Phys. Rev. Lett.* **88**, 180403 (2002).
- [35] K. Kasamatsu, M. Tsubota, and M. Ueda, Vortex phase diagram in rotating two-component Bose-Einstein condensates, *Phys. Rev. Lett.* **91**, 150406 (2003).
- [36] W.-M. Liu and E. Kengne, *Schrödinger Equations in Nonlinear Systems* (Springer Singapore, 2019).
- [37] See Supplemental Material for details about the derivation of the hydrodynamic SPE, the numerical method for solving the SPE, and additional numerical results.
- [38] J. M. Greene, Reconnection of vorticity lines and magnetic lines, *Phys. Fluids B* **5**, 2355 (1993).
- [39] M. Huang, T. Küpper, and N. Masbaum, Computation of invariant tori by the Fourier methods, *SIAM J. Sci. Comput.* **18**, 918 (1997).
- [40] J. Hao, S. Xiong, and Y. Yang, Tracking vortex surfaces frozen in the virtual velocity in non-ideal flows, *J. Fluid Mech.* **863**, 513 (2019).

- [41] Z. Meng and Y. Yang, Lagrangian dynamics and regularity of the spin Euler equation (2023), arXiv:2311.05149.
- [42] B. H. Bransden and C. J. Joachain, *Physics of Atoms and Molecules* (Pearson Education India, 2003).
- [43] Y. Ashida, Z. Gong, and M. Ueda, Non-Hermitian physics, *Adv. Phys.* **69**, 249 (2021).
- [44] G. I. Taylor and A. E. Green, Mechanism of the production of small eddies from large ones, *Proc. R. Soc. London Ser. A-Math. Phys. Eng. Sci.* **158**, 499 (1937).
- [45] S. Lloyd, G. D. Palma, C. Gokler, B. Kiani, Z.-W. Liu, M. Marvian, F. Tennie, and T. Palmer, Quantum algorithm for nonlinear differential equations (2020), arXiv:2011.06571.
- [46] N. P. Müller, J. I. Polanco, and G. Krstulovic, Intermittency of velocity circulation in quantum turbulence, *Phys. Rev. X* **11**, 011053 (2021).
- [47] W. Shen, J. Yao, and Y. Yang, Weaving classical turbulence with quantum skeleton (2024), arXiv:2401.11149.
- [48] Y. Yang, S. Xiong, and Z. Lu, Applications of the vortex-surface field to flow visualization, modelling and simulation, *Flow* **3**, E33 (2023).
- [49] E. J. Bergholtz, J. C. Budich, and F. K. Kunst, Exceptional topology of non-Hermitian systems, *Rev. Mod. Phys.* **93**, 015005 (2021).
- [50] K. Ding, C. Fang, and G. Ma, Non-Hermitian topology and exceptional-point geometries, *Nat. Rev. Phys.* **4**, 745 (2022).

# Supplementary Material for “Quantum spin representation for the Navier-Stokes equation”

Zhaoyuan Meng<sup>1</sup> and Yue Yang<sup>1,2,\*</sup>

<sup>1</sup> *State Key Laboratory for Turbulence and Complex Systems,  
College of Engineering, Peking University, Beijing 100871, PR China*

<sup>2</sup> *HEDPS-CAPT, Peking University, Beijing 100871, PR China*

\* yyg@pku.edu.cn

## CONTENTS

1.	Schrödinger-Pauli formulation of the Navier-Stokes equation	S1
	A. Derivation of the Schrödinger-Pauli equation for 3D compressible flows	S1
	B. Derivation of the Schrödinger-Pauli equation for 3D incompressible flows	S6
	C. Numerical simulation	S7
2.	Schrödinger-Pauli formulation of the 1D Burgers equation	S8
	A. Derivation of the Schrödinger-Pauli equation for a 1D compressible flow	S8
	B. Numerical simulation	S10
	References	S11

## 1. SCHRÖDINGER-PAULI FORMULATION OF THE NAVIER-STOKES EQUATION

### A. Derivation of the Schrödinger-Pauli equation for 3D compressible flows

We derive the Schrödinger-Pauli equation (SPE) which is equivalent to the Navier-Stokes equation (NSE) for general 3D flows. To incorporate the finite vorticity  $\boldsymbol{\omega} \equiv \nabla \times \mathbf{u}$  into the hydrodynamic representation of the SPE, we employ a two-component wave function as a quaternion

$$\boldsymbol{\psi}(\mathbf{x}, t) = a(\mathbf{x}, t) + b(\mathbf{x}, t)\mathbf{i} + c(\mathbf{x}, t)\mathbf{j} + d(\mathbf{x}, t)\mathbf{k} \quad (\text{S1})$$

with the basis vectors  $\{\mathbf{i}, \mathbf{j}, \mathbf{k}\}$  of the imaginary part of the quaternion and real-valued functions  $a, b, c$ , and  $d$ . This quaternion, equivalent to the two-component spinor, facilitates deriving the hydrodynamic SPE below.

The probability current is defined as [S1]

$$\mathbf{J} \equiv \frac{\hbar}{2m} (\nabla \bar{\boldsymbol{\psi}} \mathbf{i} \boldsymbol{\psi} - \bar{\boldsymbol{\psi}} \mathbf{i} \nabla \boldsymbol{\psi}) \quad (\text{S2})$$

where  $\hbar$  is the Planck constant,  $m$  the particle mass, and  $\bar{\boldsymbol{\psi}}$  the quaternion conjugate of  $\boldsymbol{\psi}$ . The flow velocity is then defined as

$$\mathbf{u} \equiv \frac{\mathbf{J}}{\rho} = \frac{\hbar}{2m} \frac{\nabla \bar{\boldsymbol{\psi}} \mathbf{i} \boldsymbol{\psi} - \bar{\boldsymbol{\psi}} \mathbf{i} \nabla \boldsymbol{\psi}}{\bar{\boldsymbol{\psi}} \boldsymbol{\psi}}, \quad (\text{S3})$$

where  $\rho \equiv \bar{\boldsymbol{\psi}} \boldsymbol{\psi}$  is the fluid density.

We propose a nonlinear SPE that is equivalent to the NSE as

$$i\hbar \frac{\partial \boldsymbol{\psi}}{\partial t} = -\frac{\hbar^2}{2m} (1 - i\nu') \Delta \boldsymbol{\psi} + \mathbf{V} \boldsymbol{\psi} - \frac{\hbar^2}{4m\rho} \mathbf{i} \boldsymbol{\psi} \Delta \mathbf{s} + \hbar \mathbf{i} \boldsymbol{\psi} \mathbf{f}, \quad (\text{S4})$$

where  $\Delta$  is the Laplacian operator,  $\nu' > 0$  serves as an effective viscosity,  $\mathbf{V} = V_1 + V_2 \mathbf{i}$  is a quaternion with two real-valued functions  $V_1$  and  $V_2$  to be determined,  $\mathbf{s} \equiv \bar{\boldsymbol{\psi}} \mathbf{i} \boldsymbol{\psi} = (a^2 + b^2 - c^2 - d^2)\mathbf{i} + 2(bc - ad)\mathbf{j} + 2(ac + bd)\mathbf{k}$  is a pure quaternion for the spin vector in  $\mathbb{R}^3$ , and  $\mathbf{f} = f_1 \mathbf{i} + f_2 \mathbf{j} + f_3 \mathbf{k}$  is a pure quaternion to be determined.

The choice of the present SPE form in Eq. (S4) is explained below. The first term on the right-hand side (RHS) involves the imaginary diffusion [S2], which accounts for the proper viscous dissipation in Newtonian fluids. The

$i$ -component  $V_2$  of the potential  $\mathbf{V}$  is employed to preserve the particle number. The last two terms on the RHS of Eq. (S4) cancel the artificial body force in the momentum equation (e.g. the Landau-Lifshitz force [S1]).

Combining Eqs. (S3) and (S4), we have

$$\begin{aligned}
\frac{\partial \rho}{\partial t} + \nabla \cdot (\rho \mathbf{u}) &= \left( \frac{\partial \bar{\psi}}{\partial t} + \frac{\hbar}{2m} \Delta \bar{\psi} \mathbf{i} \right) \psi + \bar{\psi} \left( \frac{\partial \psi}{\partial t} - \frac{\hbar}{2m} i \Delta \psi \right) \\
&= \left[ \frac{\hbar}{2m} \Delta \bar{\psi} (\nu' - i) + \frac{1}{\hbar} \bar{\psi} \bar{\mathbf{V}} \mathbf{i} + \frac{\hbar}{4m\rho} \Delta s \bar{\psi} - \mathbf{f} \bar{\psi} + \frac{\hbar}{2m} \Delta \bar{\psi} \mathbf{i} \right] \psi \\
&\quad + \bar{\psi} \left[ \frac{\hbar}{2m} (\nu' + i) \Delta \psi - \frac{1}{\hbar} i \mathbf{V} \psi - \frac{\hbar}{4m\rho} \psi \Delta s + \psi \mathbf{f} - \frac{\hbar}{2m} i \Delta \psi \right] \\
&= \left( \frac{\hbar \nu'}{2m} \Delta \bar{\psi} + \frac{1}{\hbar} \bar{\psi} \bar{\mathbf{V}} \mathbf{i} \right) \psi + \bar{\psi} \left( \frac{\hbar \nu'}{2m} \Delta \psi - \frac{1}{\hbar} i \mathbf{V} \psi \right) \\
&= \frac{\hbar \nu'}{2m} (\Delta \bar{\psi} \psi + \bar{\psi} \Delta \psi) + \frac{1}{\hbar} \bar{\psi} (\bar{\mathbf{V}} \mathbf{i} - i \mathbf{V}) \psi \\
&= \frac{\hbar \nu'}{2m} (\Delta \rho - 2|\nabla \psi|^2) + \frac{2}{\hbar} \rho V_2.
\end{aligned} \tag{S5}$$

To satisfy the continuity equation  $\partial \rho / \partial t + \nabla \cdot (\rho \mathbf{u}) = 0$ , we impose

$$V_2 = \frac{\hbar^2 \nu'}{4m} \frac{2|\nabla \psi|^2 - \Delta \rho}{\rho}. \tag{S6}$$

Then, we derive the momentum equation corresponding to Eq. (S4). Taking the material derivative  $D/Dt \equiv \partial/\partial t + \mathbf{u} \cdot \nabla$  of  $\mathbf{J}$  and using  $\mathbf{J} = (\hbar/m) \text{Re}[\nabla \bar{\psi} i \psi]$  yield

$$\frac{D\mathbf{J}}{Dt} = \frac{\hbar}{m} \text{Re} \left[ \frac{D\nabla \bar{\psi}}{Dt} i \psi + \nabla \bar{\psi} i \frac{D\psi}{Dt} \right]. \tag{S7}$$

Substituting the vector identity

$$\frac{D\nabla \bar{\psi}}{Dt} = \nabla \frac{D\bar{\psi}}{Dt} - \nabla \mathbf{u} \cdot \nabla \bar{\psi} \tag{S8}$$

into Eq. (S7), we obtain

$$\frac{D\mathbf{J}}{Dt} = \frac{\hbar}{m} \text{Re} \left[ \nabla \frac{D\bar{\psi}}{Dt} i \psi + \nabla \bar{\psi} i \frac{D\psi}{Dt} \right] - \rho \nabla \frac{|\mathbf{u}|^2}{2}. \tag{S9}$$

After some algebra, the convection of wave function reads

$$\mathbf{u} \cdot \nabla \psi = -\frac{\hbar}{2m} i \Delta \psi - \frac{1}{2} (\nabla \cdot \mathbf{u}) \psi + \frac{\hbar}{4m\rho} \left( 2|\nabla \psi|^2 i \psi - \frac{\psi}{\rho} \nabla \rho \cdot \nabla s + \psi \Delta s \right). \tag{S10}$$

Combining Eqs. (S4) and (S10), we have

$$\frac{D\psi}{Dt} = \frac{\hbar \nu'}{2m} \Delta \psi - \frac{1}{\hbar} i \mathbf{V} \psi - \frac{\hbar}{4m\rho} \psi \Delta s + \psi \mathbf{f} - \frac{1}{2} (\nabla \cdot \mathbf{u}) \psi + \frac{\hbar}{4m\rho} \left( 2|\nabla \psi|^2 i \psi - \frac{\psi}{\rho} \nabla \rho \cdot \nabla s + \psi \Delta s \right). \tag{S11}$$



Substituting Eq. (S11) with its complex conjugate into Eq. (S9) yields

$$\begin{aligned}
\frac{D\mathbf{J}}{Dt} &= -\rho(\nabla \cdot \mathbf{u})\mathbf{u} - \frac{\hbar^2}{4m^2}\nabla \left[ \frac{1}{\rho}(|\nabla\rho|^2 - \mathbf{s} \cdot \Delta\mathbf{s}) \right] + \frac{\hbar^2}{4m^2\rho^2}\nabla\rho \cdot [\nabla(\rho\nabla\rho) - \nabla\nabla\mathbf{s} \cdot \mathbf{s}] \\
&\quad - \frac{\hbar^2}{4m^2\rho}\nabla\mathbf{s} \cdot \Delta\mathbf{s} + \frac{\hbar^2}{2m^2\rho}\rho\nabla\frac{|\nabla\psi|^2}{\rho} - \rho\nabla\frac{|\mathbf{u}|^2}{2} + \frac{\hbar}{m}\text{Re}[-\nabla\mathbf{f}\bar{\psi}i\psi - \mathbf{f}\nabla\bar{\psi}i\psi + \nabla\bar{\psi}i\psi] \\
&\quad + \text{Re} \left[ \frac{\hbar^2\nu'}{2m^2}\nabla\Delta\bar{\psi}i\psi - \frac{1}{m}(\nabla\bar{\psi}\bar{V} + \bar{\psi}\nabla\bar{V})\psi + \frac{\hbar^2\nu'}{2m^2}\nabla\bar{\psi}i\Delta\psi + \frac{1}{m}\nabla\bar{\psi}V\psi \right] \\
&\quad + \frac{\hbar^2}{4m^2}\text{Re} \left[ -\frac{1}{\rho^2}\nabla\rho\Delta\mathbf{s}\bar{\psi}i\psi + \frac{1}{\rho}(\nabla\Delta\mathbf{s}\bar{\psi} + \Delta\mathbf{s}\nabla\bar{\psi})i\psi - \frac{1}{\rho}\nabla\bar{\psi}i\psi\Delta\mathbf{s} + 2\Delta\bar{\psi}i\psi\nabla\nu' \right] \\
&= -\rho(\nabla \cdot \mathbf{u})\mathbf{u} - \frac{\hbar^2}{4m^2}\nabla \left[ \frac{1}{\rho}(|\nabla\rho|^2 - \mathbf{s} \cdot \Delta\mathbf{s}) \right] + \frac{\hbar^2}{4m^2\rho^2}\nabla\rho \cdot [\nabla(\rho\nabla\rho) - \nabla\nabla\mathbf{s} \cdot \mathbf{s}] \\
&\quad - \frac{\hbar^2}{4m^2\rho}\nabla\mathbf{s} \cdot \Delta\mathbf{s} + \frac{\hbar^2}{2m^2\rho}\rho\nabla\frac{|\nabla\psi|^2}{\rho} - \rho\nabla\frac{|\mathbf{u}|^2}{2} + \frac{\hbar}{m}\nabla\mathbf{f} \cdot \mathbf{s} + \frac{\hbar}{2m}(\nabla \cdot \mathbf{J})\nabla\nu' \\
&\quad + \text{Re} \left[ \frac{\hbar^2\nu'}{2m^2}(\nabla\Delta\bar{\psi}i\psi + \nabla\bar{\psi}i\Delta\psi) + \frac{1}{m}(\nabla\bar{\psi}(V - \bar{V})\psi - \bar{\psi}\nabla\bar{V}\psi) \right] \\
&\quad + \frac{\hbar^2}{4m^2} \left( \frac{1}{\rho^2}\mathbf{s} \cdot \Delta\mathbf{s}\nabla\rho - \frac{1}{\rho}\nabla(\mathbf{s} \cdot \Delta\mathbf{s}) + \frac{1}{\rho}\nabla\mathbf{s} \cdot \Delta\mathbf{s} \right) \\
&= -\rho(\nabla \cdot \mathbf{u})\mathbf{u} - \frac{\hbar^2}{4m^2}\nabla \left( \frac{1}{\rho}|\nabla\rho|^2 \right) + \frac{\hbar^2}{4m^2\rho^2}\nabla\rho \cdot [\nabla(\rho\nabla\rho) - \nabla\nabla\mathbf{s} \cdot \mathbf{s}] + \frac{\hbar^2}{2m^2\rho}\rho\nabla\frac{|\nabla\psi|^2}{\rho} - \rho\nabla\frac{|\mathbf{u}|^2}{2} \\
&\quad - \frac{\rho}{m}\nabla V_1 + \frac{\hbar^2\nu'}{2m^2}\text{Re}[\nabla\Delta\bar{\psi}i\psi + \nabla\bar{\psi}i\Delta\psi] + \frac{\hbar}{m}\nabla\mathbf{f} \cdot \mathbf{s} + \frac{\hbar}{2m}(\rho\nabla \cdot \mathbf{u} + \mathbf{u} \cdot \nabla\rho)\nabla\nu' + \frac{2V_2\rho}{\hbar}\mathbf{u}.
\end{aligned} \tag{S12}$$

Taking the Laplacian of  $\mathbf{J}$ , we have

$$\begin{aligned}
\Delta\mathbf{J} &= \frac{\hbar}{2m}\Delta(\nabla\bar{\psi}i\psi - \bar{\psi}i\nabla\psi) \\
&= \frac{\hbar}{2m}(\nabla\Delta\bar{\psi}i\psi + \nabla\bar{\psi}i\Delta\psi + 2\nabla\nabla\bar{\psi} \cdot i\nabla\psi - 2\nabla\bar{\psi} \cdot i\nabla\nabla\psi - \Delta\bar{\psi}i\nabla\psi - \bar{\psi}i\nabla\Delta\psi).
\end{aligned} \tag{S13}$$

Taking the real part of Eq. (S13) and using the identities

$$\begin{cases} \text{Re}[\nabla\Delta\bar{\psi}i\psi] = -b\nabla\Delta a + a\nabla\Delta b - d\nabla\Delta c + c\nabla\Delta d, \\ \text{Re}[\nabla\bar{\psi}i\Delta\psi] = -\Delta b\nabla a + \Delta a\nabla b - \Delta d\nabla c + \Delta c\nabla d, \\ \text{Re}[\Delta\bar{\psi}i\nabla\psi] = -\Delta a\nabla b + \Delta b\nabla a - \Delta c\nabla d + \Delta d\nabla c, \\ \text{Re}[\bar{\psi}i\nabla\Delta\psi] = b\nabla\Delta a - a\nabla\Delta b + d\nabla\Delta c - c\nabla\Delta d, \\ \text{Re}[\nabla\nabla\bar{\psi} \cdot i\nabla\psi] = -\nabla b \cdot \nabla\nabla a + \nabla a \cdot \nabla\nabla b - \nabla d \cdot \nabla\nabla c + \nabla c \cdot \nabla\nabla d, \\ \text{Re}[\nabla\bar{\psi} \cdot i\nabla\nabla\psi] = -\nabla a \cdot \nabla\nabla b + \nabla b \cdot \nabla\nabla a - \nabla c \cdot \nabla\nabla d + \nabla d \cdot \nabla\nabla c, \end{cases} \tag{S14}$$

we obtain

$$\Delta\mathbf{J} = \text{Re}[\Delta\mathbf{J}] = \frac{\hbar}{m}\text{Re}[\nabla\Delta\bar{\psi}i\psi + \nabla\bar{\psi}i\Delta\psi]. \tag{S15}$$

Substituting the identity

$$\Delta\mathbf{J} = \Delta\rho\mathbf{u} + 2\nabla\rho \cdot \nabla\mathbf{u} + \rho\Delta\mathbf{u} \tag{S16}$$

and Eqs. (S6) and (S15) into Eq. (S12) yields

$$\begin{aligned}
\frac{D\mathbf{J}}{Dt} &= -\frac{\hbar^2}{4m^2}\nabla \left( \frac{1}{\rho}|\nabla\rho|^2 \right) + \rho\nabla \left( \frac{\hbar^2}{2m^2\rho}|\nabla\psi|^2 - \frac{|\mathbf{u}|^2}{2} - \frac{V_1}{m} \right) + \frac{\hbar\nu'}{2m}\rho\Delta\mathbf{u} + \frac{\hbar}{m}\nabla\mathbf{f} \cdot \mathbf{s} + \left( \frac{\hbar\nu'}{m}|\nabla\psi|^2 - \rho\nabla \cdot \mathbf{u} \right)\mathbf{u} \\
&\quad + \frac{\hbar^2}{4m^2\rho^2}\nabla\rho \cdot \left[ \nabla(\rho\nabla\rho) - \nabla\nabla\mathbf{s} \cdot \mathbf{s} + \frac{4m\nu'}{\hbar}\rho^2\nabla\mathbf{u} \right] + \frac{\hbar}{2m}(\rho\nabla \cdot \mathbf{u} + \mathbf{u} \cdot \nabla\rho)\nabla\nu'.
\end{aligned} \tag{S17}$$

Substituting Eq. (S17) into the relation  $D\mathbf{u}/Dt = (1/\rho)D\mathbf{J}/Dt + (\nabla \cdot \mathbf{u})\mathbf{u}$  and employing the identity  $\hbar^2|\nabla\mathbf{s}|^2/(8m^2\rho^2) = \hbar^2|\nabla\psi|^2/(2m^2\rho) - |\mathbf{u}|^2/2$  yield the momentum equation

$$\begin{aligned} \frac{D\mathbf{u}}{Dt} = & -\frac{\hbar^2}{4m^2\rho}\nabla\left(\frac{1}{\rho}|\nabla\rho|^2\right) + \nabla\left(\frac{\hbar^2}{2m^2\rho}|\nabla\psi|^2 - \frac{|\mathbf{u}|^2}{2} - \frac{V_1}{m} + \frac{\hbar}{m\rho}\mathbf{s}\cdot\mathbf{f}\right) + \frac{\hbar\nu'}{2m}\Delta\mathbf{u} + \frac{\hbar\mathbf{s}\cdot\mathbf{f}}{m\rho^2}\nabla\rho - \frac{\hbar}{m\rho}\nabla\mathbf{s}\cdot\mathbf{f} \\ & + \frac{\hbar\nu'}{m\rho}|\nabla\psi|^2\mathbf{u} + \frac{\hbar^2}{4m^2\rho^3}\nabla\rho\cdot\left[\nabla(\rho\nabla\rho) - \nabla\nabla\mathbf{s}\cdot\mathbf{s} + \frac{4m\nu'}{\hbar}\rho^2\nabla\mathbf{u}\right] + \frac{\hbar}{2m}(\nabla\cdot\mathbf{u} + \mathbf{u}\cdot\nabla\ln\rho)\nabla\nu'. \end{aligned} \quad (\text{S18})$$

To make Eq. (S18) consistent with the NSE, we set

$$V_1 = \tilde{p} + \frac{\hbar^2}{2m\rho}|\nabla\psi|^2, \quad \nu' = \frac{2m\mu}{\hbar\rho}, \quad (\text{S19})$$

with a modified pressure

$$\tilde{p} = \int \frac{m}{\rho} d\left(p - \frac{\hbar^2}{4m^2\rho}|\nabla\rho|^2 - \frac{\mu}{3}\nabla\cdot\mathbf{u}\right) - \frac{m}{2}|\mathbf{u}|^2 + \frac{\hbar}{\rho}\mathbf{s}\cdot\mathbf{f}, \quad (\text{S20})$$

where  $p$  denotes the static pressure determined by the equation of state, and  $\mu$  the viscosity.

Moreover, the vector  $\mathbf{f}$  to be determined satisfies

$$\frac{\mathbf{s}\cdot\mathbf{f}}{\rho}\nabla\rho - \nabla\mathbf{s}\cdot\mathbf{f} + \mathbf{S} = \mathbf{0}, \quad (\text{S21})$$

with

$$\mathbf{S} = \frac{2m\mu}{\hbar\rho}|\nabla\psi|^2\mathbf{u} + \frac{\hbar}{4m\rho^2}\nabla\rho\cdot\left[\nabla(\rho\nabla\rho) - \nabla\nabla\mathbf{s}\cdot\mathbf{s} + \frac{8m^2\mu}{\hbar^2}\rho\nabla\mathbf{u}\right] - \frac{m\mu}{\hbar}(\nabla\cdot\mathbf{u} + \mathbf{u}\cdot\nabla\ln\rho)\nabla\ln\rho. \quad (\text{S22})$$

Introducing the coefficient matrix

$$\mathbf{A} = \begin{bmatrix} \partial_x s_1 - s_1 \partial_x \ln \rho & \partial_x s_2 - s_2 \partial_x \ln \rho & \partial_x s_3 - s_3 \partial_x \ln \rho \\ \partial_y s_1 - s_1 \partial_y \ln \rho & \partial_y s_2 - s_2 \partial_y \ln \rho & \partial_y s_3 - s_3 \partial_y \ln \rho \\ \partial_z s_1 - s_1 \partial_z \ln \rho & \partial_z s_2 - s_2 \partial_z \ln \rho & \partial_z s_3 - s_3 \partial_z \ln \rho \end{bmatrix}, \quad (\text{S23})$$

we recast Eq. (S21) as a linear system  $\mathbf{A}[f_1 \ f_2 \ f_3]^T = [\mathcal{S}_x \ \mathcal{S}_y \ \mathcal{S}_z]^T$ . As

$$s_j \partial_i s_j - s_j s_j \partial_i \ln \rho = \rho \partial_i \rho - \rho^2 \frac{\partial_i \rho}{\rho} = 0, \quad i = 1, 2, 3, \quad (\text{S24})$$

the column rank of  $\mathbf{A}$  is not full and  $\mathbf{A}$  is non-invertible, so the solution to Eq. (S21) is not unique. We adopt the solution

$$[f_1 \ f_2 \ f_3]^T = \mathbf{A}^T(\mathbf{A}\mathbf{A}^T)^{-1}[\mathcal{S}_x \ \mathcal{S}_y \ \mathcal{S}_z]^T, \quad (\text{S25})$$

where  $\mathbf{A}^+ = \mathbf{A}^T(\mathbf{A}\mathbf{A}^T)^{-1}$  is the Moore-Penrose pseudoinverse of  $\mathbf{A}$ , which avoids the singularity for  $|\mathbf{A}| = 0$  and minimizes  $\|\mathbf{f}\|_2$ .

In sum, we recast the NSE with constant  $\mu$

$$\begin{cases} \frac{\partial\rho}{\partial t} + \nabla\cdot(\rho\mathbf{u}) = 0, \\ \frac{\partial\mathbf{u}}{\partial t} + \mathbf{u}\cdot\nabla\mathbf{u} = -\frac{1}{\rho}\nabla p + \frac{\mu}{3\rho}\nabla(\nabla\cdot\mathbf{u}) + \frac{\mu}{\rho}\Delta\mathbf{u} \end{cases} \quad (\text{S26})$$

into a nonlinear SPE in the quaternion form

$$i\hbar\frac{\partial\psi}{\partial t} = -\frac{\hbar^2}{2m}\left(1 - i\frac{2m\mu}{\hbar\rho}\right)\Delta\psi + \left(\tilde{p} + \frac{\hbar^2}{2m\rho}|\nabla\psi|^2\right)\psi + \frac{\hbar\mu}{2}\frac{2|\nabla\psi|^2 - \Delta\rho}{\rho^2}i\psi - \frac{\hbar^2}{4m\rho}i\psi\Delta\mathbf{s} + \hbar i\psi\mathbf{f}. \quad (\text{S27})$$

By introducing the two-component wave function  $|\psi_{\pm}\rangle = [\psi_+, \psi_-]^T$  with  $\psi_+ = a + ib$  and  $\psi_- = c + id$ , we rewrite Eq. (S27) into

$$\begin{aligned} i\hbar \frac{\partial}{\partial t} \begin{bmatrix} \psi_+ \\ \psi_- \end{bmatrix} &= \left[ \left( 1 - i \frac{2m\mu}{\hbar\rho} \right) \frac{\hat{\mathbf{p}}^2}{2m} + \tilde{p} + \frac{\hbar^2}{2m\rho} |\nabla\psi_{\pm}|^2 + i \frac{\hbar\mu}{2} \frac{2|\nabla\psi_{\pm}|^2 - \Delta\rho}{\rho^2} \right] \begin{bmatrix} \psi_+ \\ \psi_- \end{bmatrix} \\ &+ \begin{bmatrix} \frac{\hbar^2\Delta s_1}{4m\rho} - \hbar f_1 & \frac{\hbar^2(\Delta s_3 + i\Delta s_2)}{4m\rho} - \hbar(f_3 + if_2) \\ \frac{\hbar^2(\Delta s_3 - i\Delta s_2)}{4m\rho} - \hbar(f_3 - if_2) & -\frac{\hbar^2\Delta s_1}{4m\rho} + \hbar f_1 \end{bmatrix} \begin{bmatrix} \psi_+ \\ \psi_- \end{bmatrix}, \end{aligned} \quad (\text{S28})$$

where  $\hat{\mathbf{p}}$  is the momentum operator, and the spin-vector components in terms of  $\psi_{\pm}$  are

$$\begin{cases} s_1 = |\psi_+|^2 - |\psi_-|^2, \\ s_2 = i(\psi_+^* \psi_- - \psi_+ \psi_-^*), \\ s_3 = \psi_+^* \psi_- + \psi_+ \psi_-^*. \end{cases} \quad (\text{S29})$$

By introducing the Pauli vector

$$\boldsymbol{\sigma} = \sigma_1 \mathbf{e}_1 + \sigma_2 \mathbf{e}_2 + \sigma_3 \mathbf{e}_3 = \begin{bmatrix} 0 & 1 \\ 1 & 0 \end{bmatrix} \mathbf{e}_1 + \begin{bmatrix} 0 & -i \\ i & 0 \end{bmatrix} \mathbf{e}_2 + \begin{bmatrix} 1 & 0 \\ 0 & -1 \end{bmatrix} \mathbf{e}_3, \quad (\text{S30})$$

Eq. (S28) becomes

$$i\hbar \frac{\partial}{\partial t} |\psi_{\pm}\rangle = \left[ \left( 1 - i \frac{2m\mu}{\hbar\rho} \right) \frac{\hat{\mathbf{p}}^2}{2m} + \tilde{p} + \frac{\hbar^2}{2m\rho} |\nabla\psi_{\pm}|^2 + i \frac{\hbar\mu}{2} \frac{2|\nabla\psi_{\pm}|^2 - \Delta\rho}{\rho^2} \right] \mathbf{I} |\psi_{\pm}\rangle + \boldsymbol{\sigma} \cdot \mathbf{B} |\psi_{\pm}\rangle, \quad (\text{S31})$$

with the  $2 \times 2$  identity matrix  $\mathbf{I}$ , and

$$\mathbf{B} = \mathbf{T}_0 \cdot \tilde{\mathbf{B}}, \quad \tilde{\mathbf{B}} = \frac{\hbar^2}{4m\rho} \Delta \mathbf{s} - \hbar \mathbf{f}, \quad \mathbf{T}_0 = \begin{bmatrix} 0 & 0 & 1 \\ 0 & -1 & 0 \\ 1 & 0 & 0 \end{bmatrix}. \quad (\text{S32})$$

After some algebra, we obtain the energy expectation of Eq. (S31) as

$$\langle E \rangle = \int_{\mathcal{D}} \left[ \frac{m\rho |\mathbf{u}|^2}{2} + \rho P + \frac{\hbar^2}{4m} \left( \Delta\rho + \frac{|\nabla\rho|^2}{\rho} \right) \right] d\mathbf{x} + i\hbar\mu \int_{\mathcal{D}} \mathbf{u} \cdot \nabla \ln \rho d\mathbf{x}. \quad (\text{S33})$$

For the inviscid flow with  $\mu = 0$ , Eq. (S26) degenerates to the compressible Euler equations

$$\begin{cases} \frac{\partial \rho}{\partial t} + \nabla \cdot (\rho \mathbf{u}) = 0, \\ \frac{\partial \mathbf{u}}{\partial t} + \mathbf{u} \cdot \nabla \mathbf{u} = -\frac{1}{\rho} \nabla p, \end{cases} \quad (\text{S34})$$

and the corresponding SPE reduces to

$$i\hbar \frac{\partial}{\partial t} |\psi_{\pm}\rangle = \left( \frac{\hat{\mathbf{p}}^2}{2m} + \tilde{p} + \frac{\hbar^2}{2m\rho} |\nabla\psi_{\pm}|^2 \right) \mathbf{I} |\psi_{\pm}\rangle + \boldsymbol{\sigma} \cdot \mathbf{B} |\psi_{\pm}\rangle, \quad (\text{S35})$$

with the modified pressure

$$\tilde{p} = \int \frac{m}{\rho} d \left( p - \frac{\hbar^2}{4m^2\rho} |\nabla\rho|^2 \right) - \frac{m}{2} |\mathbf{u}|^2 + \frac{\hbar}{\rho} \mathbf{s} \cdot \mathbf{f}, \quad (\text{S36})$$

and  $\mathbf{f} = \mathbf{A}^T (\mathbf{A} \mathbf{A}^T)^{-1} \cdot \mathbf{S}$  with  $\mathbf{A}$  in Eq. (S23) and

$$\mathbf{S} = \frac{\hbar}{4m\rho^2} \nabla\rho \cdot [\nabla(\rho \nabla\rho) - \nabla \nabla \mathbf{s} \cdot \mathbf{s}]. \quad (\text{S37})$$

### B. Derivation of the Schrödinger-Pauli equation for 3D incompressible flows

We consider the incompressible flow with constant density  $\rho = \rho_0$ . This flow is described by a special form of the SPE in Eq. (S31). To derive this SPE, Eq. (S18) can be simplified as

$$\frac{D\mathbf{u}}{Dt} = \nabla \left( \frac{\hbar^2}{2m^2\rho_0} |\nabla\psi|^2 - \frac{|\mathbf{u}|^2}{2} - \frac{V_1}{m} \right) + \frac{\hbar\nu'}{2m} \Delta\mathbf{u} + \frac{\hbar}{m\rho_0} \nabla\mathbf{f} \cdot \mathbf{s} + \frac{\hbar\nu'}{m\rho_0} |\nabla\psi|^2 \mathbf{u}. \quad (\text{S38})$$

Then, we specify  $\nu' = 2m\nu/\hbar$  and enforce

$$\nabla \left( \frac{\hbar^2}{2m^2\rho_0} |\nabla\psi|^2 - \frac{|\mathbf{u}|^2}{2} - \frac{V_1}{m} \right) + \frac{\hbar}{m\rho_0} \nabla\mathbf{f} \cdot \mathbf{s} + \frac{2\nu}{\rho_0} |\nabla\psi|^2 \mathbf{u} = -\nabla \frac{p}{\rho_0}, \quad (\text{S39})$$

where  $\nu \equiv \mu/\rho_0$  is the kinematic viscosity. Applying the identity  $\nabla\mathbf{f} \cdot \mathbf{s} = \nabla(\mathbf{f} \cdot \mathbf{s}) - \nabla\mathbf{s} \cdot \mathbf{f}$  to Eq. (S39) yields

$$\frac{\hbar}{m\rho_0} \nabla\mathbf{s} \cdot \mathbf{f} - \frac{2\nu}{\rho_0} |\nabla\psi|^2 \mathbf{u} = \nabla\phi_h, \quad (\text{S40})$$

where

$$\phi_h \equiv \frac{p}{\rho_0} + \frac{\hbar^2}{2m^2\rho_0} |\nabla\psi|^2 - \frac{|\mathbf{u}|^2}{2} - \frac{V_1}{m} + \frac{\hbar}{m\rho_0} \mathbf{s} \cdot \mathbf{f} \quad (\text{S41})$$

is a real-valued function to be determined.

Projecting Eq. (S40) onto  $\boldsymbol{\omega}$  and using the identity  $\boldsymbol{\omega} \cdot \nabla\mathbf{s} = \mathbf{0}$ , we find

$$\boldsymbol{\omega} \cdot \nabla\phi_h = -\frac{2\nu}{\rho_0} |\nabla\psi|^2 h, \quad (\text{S42})$$

where  $h \equiv \mathbf{u} \cdot \boldsymbol{\omega}$  denotes the helicity density. We rewrite Eq. (S41) into

$$V_1 = \tilde{p} + \frac{\hbar^2}{2m\rho_0} |\nabla\psi|^2, \quad (\text{S43})$$

with a modified pressure

$$\tilde{p} = m \left( \frac{p}{\rho_0} - \frac{|\mathbf{u}|^2}{2} - \phi_h \right) + \frac{\hbar}{\rho_0} \mathbf{s} \cdot \mathbf{f}. \quad (\text{S44})$$

Here,  $\mathbf{f}$  is given by Eq. (S25) with

$$\mathbf{A} = \begin{bmatrix} \partial_x s_1 & \partial_x s_2 & \partial_x s_3 \\ \partial_y s_1 & \partial_y s_2 & \partial_y s_3 \\ \partial_z s_1 & \partial_z s_2 & \partial_z s_3 \end{bmatrix} \quad (\text{S45})$$

and

$$\mathbf{S} = \frac{2m\nu}{\hbar} |\nabla\psi|^2 \mathbf{u} - \frac{m\rho_0}{\hbar} \nabla\phi_h. \quad (\text{S46})$$

In sum, we reformulate the incompressible NSE

$$\begin{cases} \nabla \cdot \mathbf{u} = 0, \\ \frac{\partial \mathbf{u}}{\partial t} + \mathbf{u} \cdot \nabla \mathbf{u} = -\nabla \frac{p}{\rho_0} + \nu \Delta \mathbf{u} \end{cases} \quad (\text{S47})$$

into a nonlinear SPE in the quaternion form

$$i\hbar \frac{\partial \psi}{\partial t} = -\frac{\hbar^2}{2m} \left( 1 - i \frac{2m\nu}{\hbar} \right) \Delta \psi + \left( \tilde{p} + \frac{\hbar^2}{2m\rho_0} |\nabla\psi|^2 + \frac{\hbar\nu}{\rho_0} |\nabla\psi|^2 i \right) \psi - \frac{\hbar^2}{4m\rho_0} i\psi \Delta \mathbf{s} + \hbar i\psi \mathbf{f}. \quad (\text{S48})$$

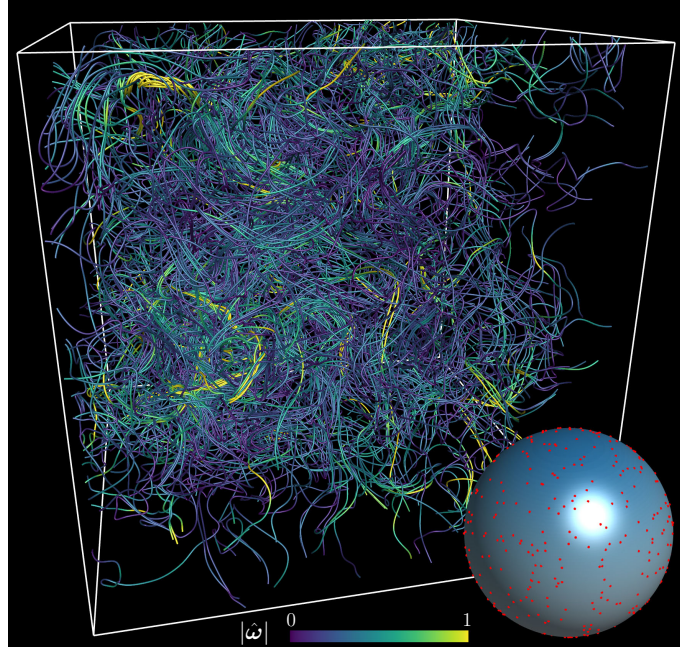


FIG. S1. Tangle of vortex lines color-coded by the normalized vorticity magnitude  $|\hat{\omega}| \equiv |\omega|/|\omega|_{\max}$  in homogeneous isotropic turbulence. Each vortex line maps to a red point on the Bloch sphere  $\mathbb{S}^2$  through the spherical Clebsch mapping.

Similarly, Eq. (S48) is re-expressed in terms of  $\psi_{\pm}$  as

$$i\hbar \frac{\partial}{\partial t} |\psi_{\pm}\rangle = \left[ \left(1 - i\frac{2m\nu}{\hbar}\right) \frac{\hat{\mathbf{p}}^2}{2m} + \tilde{p} + \frac{\hbar^2}{2m\rho_0} |\nabla\psi_{\pm}|^2 + i\frac{\hbar\nu}{\rho_0} |\nabla\psi_{\pm}|^2 \right] \mathbf{I}|\psi_{\pm}\rangle + \boldsymbol{\sigma} \cdot \mathbf{B}|\psi_{\pm}\rangle, \quad (\text{S49})$$

with  $\mathbf{B} = \mathbf{T}_0 \cdot [\hbar^2 \Delta \mathbf{s}/(4m\rho_0) - \hbar \mathbf{f}]$ . After some algebra, we obtain the energy expectation of Eq. (S49) as

$$\langle E \rangle = m\rho_0 \int_{\mathcal{D}} \left( \frac{|\mathbf{u}|^2}{2} + \frac{p}{\rho_0} - \phi_h \right) d\mathbf{x}. \quad (\text{S50})$$

Note that  $\mathbf{f}$  has an exact expression for 3D compressible flows, whereas in general  $\mathbf{f}$  cannot be determined for incompressible flows. This implies that incompressible viscous flow corresponds to a peculiar quantum system. The quantum system in Eq. (S49) always has a real-valued energy expectation in Eq. (S50), unlike the possible complex values in compressible flows.

For the incompressible flow, the NSE-SPE mapping exhibits a remarkable geometric feature – it transforms the vorticity, a solenoidal vector field in  $\mathbb{R}^3$ , into a spin vector in  $\mathbb{S}^2$ . Namely, each vortex line in space  $\mathbb{R}^3$  is associated with a point on the Bloch sphere [S3–S5], as illustrated in Fig. (S1).

For  $\nu = 0$ , Eq. (S47) reduces to the incompressible Euler equations

$$\begin{cases} \nabla \cdot \mathbf{u} = 0, \\ \frac{\partial \mathbf{u}}{\partial t} + \mathbf{u} \cdot \nabla \mathbf{u} + \nabla \frac{p}{\rho_0} = \mathbf{0}. \end{cases} \quad (\text{S51})$$

With  $\mathbf{f} = \mathbf{0}$  and  $\phi_h = 0$ , the corresponding SPE simplifies to

$$i\hbar \frac{\partial}{\partial t} |\psi_{\pm}\rangle = \left( \frac{\hat{\mathbf{p}}^2}{2m} + \tilde{p} + \frac{\hbar^2}{2m\rho_0} |\nabla\psi_{\pm}|^2 \right) \mathbf{I}|\psi_{\pm}\rangle + \boldsymbol{\sigma} \cdot \mathbf{B}|\psi_{\pm}\rangle \quad (\text{S52})$$

with  $\tilde{p} = m(p/\rho_0 - |\mathbf{u}|^2/2)$  and  $\mathbf{B} = \mathbf{T}_0 \cdot [\hbar^2 \Delta \mathbf{s}/(4m\rho_0)]$ .

### C. Numerical simulation

We develop a numerical algorithm to solve Eq. (S31) for compressible flows and Eq. (S49) for incompressible, constant-density flows with  $\rho_0 = 1$ . Here we set  $m = 1$  and  $\hbar = 1$  without loss of generality.

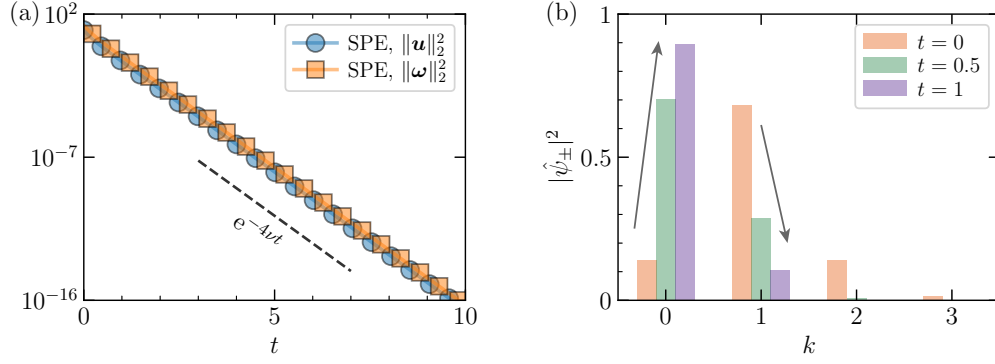


FIG. S2. (a) Total kinetic energy  $\|\mathbf{u}\|_2^2$  and enstrophy  $\|\boldsymbol{\omega}\|_2^2$  of the 2D TG flow simulated by Eq. (9). Both decay exponentially as predicted by the exact solution. (b) Momentum representation of the wave function probability distribution at  $t = 0, 0.5$ , and 1. The particle evolves into the zero momentum state with time.

The solution domain  $\mathcal{D} = [0, 2\pi]^d$  with the space dimension  $d$  and periodic boundary condition is discretized on  $N^d$  uniform grid points. We employ the fraction-step Fourier method based on the second-order Trotter-Suzuki decomposition [S6, S7] for time integration. For compressible flows, we directly compute the modified pressure by integrating the static pressure from the equation of state. For incompressible flows, we project a temporary wave function onto a divergence-free subspace, instead of solving the pressure-Poisson equation to calculate the pressure.

The numerical method is presented in Algorithm 1, where  $\mathbf{k} = (k_1, \dots, k_d)$  is the  $d$ -dimensional wavenumber vector with  $k_i = -N/2, -N/2 + 1, \dots, N/2 - 1$ ,  $i = 1, 2, \dots, d$ ,  $k = |\mathbf{k}|$  is the wavenumber magnitude, and  $\mathcal{F}$  and  $\mathcal{F}^{-1}$  represent the Fourier transform and its inverse, respectively. The superscripts  $n$  and  $n + 1$  correspond to the time steps at  $t$  and  $t + \Delta t$ , respectively.

We simulate the incompressible 2D Taylor-Green (TG) viscous flow by solving Eq. (9) with  $\nu = 1$ . The exact solutions for the velocity and vorticity are  $\mathbf{u}(\mathbf{x}, t) = e^{-2\nu t}(\sin x \cos y \mathbf{e}_x - \cos x \sin y \mathbf{e}_y)$  and  $\boldsymbol{\omega}_z(\mathbf{x}, t) = 2e^{-2\nu t} \sin x \sin y$ , respectively, with the Cartesian unit vectors  $\{\mathbf{e}_x, \mathbf{e}_y\}$ . The initial wave function is

$$\begin{cases} \psi_+(\mathbf{x}, 0) = \cos \left[ \arccos \left( \cos \frac{x}{2} \right) \right] e^{i \cos y (2 - \cos x)}, \\ \psi_-(\mathbf{x}, 0) = \sin \left[ \arccos \left( \cos \frac{x}{2} \right) \right] e^{-i \cos y (2 + \cos x)}. \end{cases} \quad (\text{S53})$$

The numerical result exhibits an excellent agreement with the exact solution in Fig. S2(a) – the total kinetic energy  $\|\mathbf{u}\|_2^2$  and enstrophy  $\|\boldsymbol{\omega}\|_2^2$  decay exponentially. In Fig. S2(b), the peak of the wave-function probability distribution migrates towards the zero-momentum state with time.

## 2. SCHRÖDINGER-PAULI FORMULATION OF THE 1D BURGERS EQUATION

### A. Derivation of the Schrödinger-Pauli equation for a 1D compressible flow

We derive the SPE equivalent to the Burgers equation

$$u_t + uu_x = \nu u_{xx}. \quad (\text{S54})$$

---

**Algorithm 1:** Time iteration for solving the SPE for fluid flows.

---

**Input:**  $|\psi_{\pm}(t)\rangle$ ,  $\mu$  (or  $\nu$ ),  $\Delta t$ ,  $N$   
**Output:**  $|\psi_{\pm}(t + \Delta t)\rangle$

- 1  $\psi_{\pm}^n(\mathbf{x}) \leftarrow |\psi_{\pm}(t)\rangle$ ;
- 2 Calculate the spin vector  $\mathbf{s}^n(\mathbf{x})$  by Eq. (5);
- 3 **if** *compressible* **then**
- 4     Calculate the fluid density  $\rho^n(\mathbf{x})$  by Eq. (2);
- 5     Calculate the velocity  $\mathbf{u}^n(\mathbf{x})$  by Eq. (1);
- 6     Calculate the coefficient matrix  $\mathbf{A}^n(\mathbf{x})$  by Eq. (S23);
- 7     **if** *viscous* **then**
- 8         Calculate the source term  $\mathcal{S}^n(\mathbf{x})$  by Eq. (S22);
- 9         Calculate  $\mathbf{f}^n(\mathbf{x})$  by Eq. (S25);
- 10         Calculate the modified pressure  $\tilde{p}^n(\mathbf{x})$  by Eq. (S20);
- 11         Calculate the real and imaginary potentials  $V_r^n(\mathbf{x}) = |\nabla\psi_{\pm}^n|^2/(2\rho^n)$  and  $V_i^n(\mathbf{x}) = \mu(2|\nabla\psi_{\pm}^n|^2 - \Delta\rho^n)/[2(\rho^n)^2]$ ;
- 12         Calculate the spin-coupled potentials  $P^n(\mathbf{x}) = \Delta s_1^n/(4\rho^n) - f_1^n$  and  $Q^n(\mathbf{x}) = (\Delta s_3^n + i\Delta s_2^n)/(4\rho^n) - (f_3^n + if_2^n)$ ;
- 13          $\psi_{\pm}^*(\mathbf{x}) \leftarrow \mathcal{F}^{-1}\{e^{-(\mu/\rho^n + i/2)k^2\Delta t}\mathcal{F}\{\psi_{\pm}^n\}\}$ ;
- 14          $\psi_{\pm}^{n+1}(\mathbf{x}) \leftarrow e^{-i(\tilde{p}^n + V_r^n \pm P^n + iV_i^n)\Delta t}\psi_{\pm}^* + (e^{-i(\text{Re}[Q^n] \pm i\text{Im}[Q^n])\Delta t} - 1)\psi_{\mp}^*$ ;
- 15     **end**
- 16     **if** *inviscid* **then**
- 17         Calculate the source term  $\mathcal{S}^n(\mathbf{x})$  by Eq. (S37);
- 18         Calculate  $\mathbf{f}^n(\mathbf{x})$  by Eq. (S25);
- 19         Calculate the modified pressure  $\tilde{p}^n(\mathbf{x})$  by Eq. (S36);
- 20         Calculate the real potential  $V_r^n(\mathbf{x}) = |\nabla\psi_{\pm}^n|^2/(2\rho^n)$ ;
- 21         Calculate the spin-coupled potentials  $P^n(\mathbf{x}) = \Delta s_1^n/(4\rho^n) - f_1^n$  and  $Q^n(\mathbf{x}) = (\Delta s_3^n + i\Delta s_2^n)/(4\rho^n) - (f_3^n + if_2^n)$ ;
- 22          $\psi_{\pm}^*(\mathbf{x}) \leftarrow \mathcal{F}^{-1}\{e^{-ik^2\Delta t/2}\mathcal{F}\{\psi_{\pm}^n\}\}$ ;
- 23          $\psi_{\pm}^{n+1}(\mathbf{x}) \leftarrow e^{-i(\tilde{p}^n + V_r^n \pm P^n)\Delta t}\psi_{\pm}^* + (e^{-i(\text{Re}[Q^n] \pm i\text{Im}[Q^n])\Delta t} - 1)\psi_{\mp}^*$ ;
- 24     **end**
- 25 **end**
- 26 **if** *incompressible* **then**
- 27     Calculate the velocity  $\mathbf{u}^n(\mathbf{x})$  by Eq. (1);
- 28     **if** *viscous* **then**
- 29         Calculate the coefficient matrix  $\mathbf{A}^n(\mathbf{x})$  by Eq. (S45);
- 30         Obtain  $\phi_h^n(\mathbf{x})$  by solving Eq. (S42);
- 31         Calculate the source term  $\mathcal{S}^n(\mathbf{x})$  by Eq. (S46);
- 32         Calculate  $\mathbf{f}^n(\mathbf{x})$  by Eq. (S25);
- 33         Calculate the real and imaginary potentials  $V_r^n(\mathbf{x}) = |\nabla\psi_{\pm}^n|^2/2$  and  $V_i^n(\mathbf{x}) = \nu|\nabla\psi_{\pm}^n|^2$ ;
- 34         Calculate the spin-coupled potentials  $P^n(\mathbf{x}) = \Delta s_1^n/4 - f_1^n$  and  $Q^n(\mathbf{x}) = (\Delta s_3^n + i\Delta s_2^n)/4 - (f_3^n + if_2^n)$ ;
- 35          $\psi_{\pm}^*(\mathbf{x}) \leftarrow \mathcal{F}^{-1}\{e^{-(\nu + i/2)k^2\Delta t}\mathcal{F}\{\psi_{\pm}^n\}\}$ ;
- 36          $\psi_{\pm}^{**}(\mathbf{x}) \leftarrow e^{-i(V_r^n \pm P^n + iV_i^n)\Delta t}\psi_{\pm}^* + (e^{-i(\text{Re}[Q^n] \pm i\text{Im}[Q^n])\Delta t} - 1)\psi_{\mp}^*$ ;
- 37     **end**
- 38     **if** *inviscid* **then**
- 39         Calculate the real potential  $V_r^n(\mathbf{x}) = |\nabla\psi_{\pm}^n|^2/2$ ;
- 40         Calculate the spin-coupled potentials  $P^n(\mathbf{x}) = \Delta s_1^n/4$  and  $Q^n(\mathbf{x}) = (\Delta s_3^n + i\Delta s_2^n)/4$ ;
- 41          $\psi_{\pm}^*(\mathbf{x}) \leftarrow \mathcal{F}^{-1}\{e^{-ik^2\Delta t/2}\mathcal{F}\{\psi_{\pm}^n\}\}$ ;
- 42          $\psi_{\pm}^{**}(\mathbf{x}) \leftarrow e^{-i(V_r^n \pm P^n)\Delta t}\psi_{\pm}^* + (e^{-i(\text{Re}[Q^n] \pm i\text{Im}[Q^n])\Delta t} - 1)\psi_{\mp}^*$ ;
- 43     **end**
- 44      $\psi_{\pm}^{***}(\mathbf{x}) \leftarrow \psi_{\pm}^{**}/|\psi_{\pm}^{**}|$ ;
- 45     Obtain the phase shift  $q^n(\mathbf{x})$  by solving the Poisson equation  $\Delta q^n = \langle \Delta\psi_{\pm}^{***}, i\psi_{\pm}^{***} \rangle_{\mathbb{R}}$ ;
- 46      $\psi_{\pm}^{n+1}(\mathbf{x}) \leftarrow e^{-iq^n}\psi_{\pm}^{***}$ ;
- 47 **end**
- 48  $|\psi_{\pm}(t + \Delta t)\rangle \leftarrow \psi_{\pm}^{n+1}(\mathbf{x})$ .

---

Setting  $\nu' = 2m\nu/\hbar$ , the 1D form of Eq. (S18) reduces to

$$\begin{aligned}
u_t + uu_x &= \nu u_{xx} - \frac{\hbar^2}{4m^2\rho} \frac{\partial}{\partial x} \left( \frac{\rho_x^2}{\rho} \right) + \frac{\partial}{\partial x} \left( \frac{\hbar^2}{2m^2\rho} |\psi_x|^2 - \frac{u^2}{2} - \frac{V_1}{m} + \frac{\hbar}{m\rho} \mathbf{s} \cdot \mathbf{f} \right) + \frac{\hbar \mathbf{s} \cdot \mathbf{f}}{m\rho^2} \rho_x - \frac{\hbar}{m\rho} \mathbf{s}_x \cdot \mathbf{f} \\
&\quad + \frac{2\nu}{\rho} |\psi_x|^2 u + \frac{\hbar^2}{4m^2\rho^3} \rho_x \left[ \frac{\partial}{\partial x} (\rho \rho_x) - \mathbf{s} \cdot \mathbf{s}_{xx} + \frac{8m^2\nu}{\hbar^2} \rho^2 u_x \right] \\
&= \nu u_{xx} + \frac{\hbar \rho_x}{m\rho^2} \left[ \mathbf{s} \cdot \mathbf{f} + \frac{\hbar}{4m\rho} (\rho_x^2 - 2\rho\rho_{xx} + |\mathbf{s}_x|^2) \right] - \frac{\hbar}{m\rho} \mathbf{s}_x \cdot \mathbf{f} + \frac{2\nu}{\rho} (\rho_x u_x + |\psi_x|^2 u) \\
&\quad + \frac{\partial}{\partial x} \left( \frac{\hbar^2}{8m^2\rho^2} |\mathbf{s}_x|^2 - \frac{V_1}{m} + \frac{\hbar}{m\rho} \mathbf{s} \cdot \mathbf{f} \right).
\end{aligned} \tag{S55}$$

Subsequently, we enforce

$$\begin{cases} \mathbf{s} \cdot \mathbf{f} + \frac{\hbar}{4m\rho} (\rho_x^2 - 2\rho\rho_{xx} + |\mathbf{s}_x|^2) = 0, \\ -\frac{\hbar}{m\rho} \mathbf{s}_x \cdot \mathbf{f} + \frac{2\nu}{\rho} (\rho_x u_x + |\psi_x|^2 u) = 0, \\ \frac{\hbar^2}{8m^2\rho^2} |\mathbf{s}_x|^2 - \frac{V_1}{m} + \frac{\hbar}{m\rho} \mathbf{s} \cdot \mathbf{f} = 0. \end{cases} \tag{S56}$$

The solutions to Eq. (S56) are

$$\mathbf{f} = \lambda_1 \mathbf{s} + \lambda_2 \mathbf{s}_x, \quad V_1 = -\frac{\hbar^2}{4m\rho^2} \left( \rho_x^2 - 2\rho\rho_{xx} + \frac{1}{2} |\mathbf{s}_x|^2 \right) \tag{S57}$$

with

$$\begin{bmatrix} \lambda_1 \\ \lambda_2 \end{bmatrix} = \frac{1}{\rho^2 (|\mathbf{s}_x|^2 - \rho_x^2)} \begin{bmatrix} |\mathbf{s}_x|^2 & -\rho\rho_x \\ -\rho\rho_x & \rho^2 \end{bmatrix} \begin{bmatrix} -\frac{\hbar}{4m\rho} (\rho_x^2 - 2\rho\rho_{xx} + |\mathbf{s}_x|^2) \\ \frac{2m\nu}{\hbar} (\rho_x u_x + |\psi_x|^2 u) \end{bmatrix}. \tag{S58}$$

Hence, the equivalent SPE for the Burgers equation (S54) reads

$$i\hbar \frac{\partial}{\partial t} |\psi_{\pm}\rangle = \left[ \left( 1 - i\frac{2m\nu}{\hbar} \right) \frac{\hat{\mathbf{p}}^2}{2m} - \frac{\hbar^2}{4m\rho^2} \left( \rho_x^2 - 2\rho\rho_{xx} + \frac{1}{2} |\mathbf{s}_x|^2 \right) + i\frac{\hbar\nu(2|\psi_x|^2 - \rho_{xx})}{2\rho} \right] \mathbf{I} |\psi_{\pm}\rangle + \boldsymbol{\sigma} \cdot \mathbf{B} |\psi_{\pm}\rangle, \tag{S59}$$

with  $\mathbf{B} = \mathbf{T}_0 \cdot [\hbar^2 \mathbf{s}_{xx}/(4m\rho) - \hbar \mathbf{f}]$ .

## B. Numerical simulation

We develop a numerical algorithm for solving Eq. (S59). Here  $m = 1$  and  $\hbar = 1$  are set without loss of generality. The solution domain  $x \in \mathcal{D}$  is discretized on uniform grid points  $x_j$ ,  $j = 1, 2, \dots, N$  with mesh spacing  $\Delta x$ . The second-order central difference and the first-order backward difference are employed for the spatial discretization and time marching, respectively. The discretized Eq. (S59) reads

$$\begin{cases} i \frac{\psi_{+,j}^{n+1} - \psi_{+,j}^n}{\Delta t} = \left( i\nu - \frac{1}{2} \right) \frac{\psi_{+,j+1}^{n+1} - 2\psi_{+,j}^{n+1} + \psi_{+,j-1}^{n+1}}{\Delta x^2} + (V_j^n + iW_j^n) \psi_{+,j}^n + P_j^n \psi_{+,j}^n + Q_j^n \psi_{-,j}^n, \\ i \frac{\psi_{-,j}^{n+1} - \psi_{-,j}^n}{\Delta t} = \left( i\nu - \frac{1}{2} \right) \frac{\psi_{-,j+1}^{n+1} - 2\psi_{-,j}^{n+1} + \psi_{-,j-1}^{n+1}}{\Delta x^2} + (V_j^n + iW_j^n) \psi_{-,j}^n + (Q_j^n)^* \psi_{+,j}^n - P_j^n \psi_{-,j}^n, \end{cases} \tag{S60}$$

with the time stepping  $\Delta t$  and potentials

$$V = -\frac{\hbar^2}{4m\rho^2} \left( \rho_x^2 - 2\rho\rho_{xx} + \frac{1}{2} |\mathbf{s}_x|^2 \right), \quad W = \frac{\nu(2|\psi_x|^2 - \rho_{xx})}{2\rho}, \tag{S61}$$

and

$$P = \frac{\Delta s_1}{4\rho} - f_1, \quad Q = \frac{\Delta s_3 + i\Delta s_2}{4\rho} - (f_3 + if_2). \tag{S62}$$



We impose the Neumann boundary conditions on the wave function at the boundary as

$$\frac{\psi_{\pm,2} - \psi_{\pm,0}}{2\Delta x} = 0, \quad \frac{\psi_{\pm,N+1} - \psi_{\pm,N-1}}{2\Delta x} = 0. \quad (\text{S63})$$

Then, we obtain two linear systems

$$\begin{cases} \alpha\psi_{+,j+1}^{n+1} - (2\alpha + 1)\psi_{+,j}^{n+1} + \alpha\psi_{+,j-1}^{n+1} = i\Delta t [(V_j^n + P_j^n + iW_j^n)\psi_{+,j}^n + Q_j^n\psi_{-,j}^n] - \psi_{+,j}^n, \\ \alpha\psi_{-,j+1}^{n+1} - (2\alpha + 1)\psi_{-,j}^{n+1} + \alpha\psi_{-,j-1}^{n+1} = i\Delta t [(V_j^n - P_j^n + iW_j^n)\psi_{-,j}^n + (Q_j^n)^*\psi_{+,j}^n] - \psi_{-,j}^n \end{cases} \quad (\text{S64})$$

from Eqs. (S60) and (S63) with  $\alpha = (\nu + i/2)\Delta t/\Delta x^2$ . The tridiagonal matrix in Eq. (S64) is strictly diagonally dominant due to

$$|2\alpha + 1| = \frac{\Delta t}{\Delta x^2} \sqrt{\left(2\nu + \frac{\Delta x^2}{\Delta t}\right)^2 + 1} > \frac{\Delta t}{\Delta x^2} \sqrt{(2\nu)^2 + 1} = |2\alpha|, \quad (\text{S65})$$

so that Eq. (S64) can be numerically solved efficiently by the catch-up method. The numerical method is presented in Algorithm 2.

---

**Algorithm 2:** Time iteration of the SPE equivalent to the Burgers equation.

---

**Input:**  $|\psi_{\pm}(t)\rangle, \nu, \Delta x, \Delta t, N$   
**Output:**  $|\psi_{\pm}(t + \Delta t)\rangle$

- 1  $\psi_{\pm,j}^n \leftarrow |\psi_{\pm}(t)\rangle$ ;
- 2 **for**  $j \leftarrow 1$  **to**  $N$  **do**
- 3     Calculate the fluid density  $\rho_j^n$  by Eq. (2) and the velocity  $u_j^n$  by Eq. (1);
- 4     Calculate the spin vector  $\mathbf{s}_j^n$  by Eq. (5);
- 5     Calculate  $(\rho_x)_j^n, (\rho_{xx})_j^n, (u_x)_j^n, (\mathbf{s}_x)_j^n$ , and  $(\psi_{\pm,x})_j^n$  using second-order central difference;
- 6     Calculate  $(\lambda_1)_j^n$  and  $(\lambda_2)_j^n$  by Eq. (S58);
- 7     Calculate  $\mathbf{f}_j^n$  by Eq. (S57);
- 8     Calculate the potentials  $V_j^n, W_j^n, P_j^n$ , and  $Q_j^n$  by Eqs. (S61) and (S62);
- 9     Obtain  $\psi_{\pm,j}^{n+1}$  by solving the linear systems in Eq. (S64) using catch-up method;
- 10 **end**
- 11  $|\psi_{\pm}(t + \Delta t)\rangle \leftarrow \psi_{\pm,j}^{n+1}$ .

---

We conduct the SPE-based numerical simulation for the 1D Burgers equation

$$\begin{cases} u_t + uu_x = \nu u_{xx}, & x \in [0, 2\pi], t > 0, \\ u(x, 0) = \sin x, & u(0, t) = u(2\pi, t) = 0. \end{cases} \quad (\text{S66})$$

The initial wave function is  $\psi_+(x, 0) = \cos x e^{-i \cos x}$  and  $\psi_-(x, 0) = \sin x e^{-i \cos x}$ .

In Fig. S3(a), the velocity calculated from the SPE agrees with the exact solution

$$u(x, t) = -2\nu \frac{\sum_{k=-\infty}^{\infty} ik e^{-\nu k^2 t + ikx} \int_0^{2\pi} e^{\cos x'/(2\nu)} e^{-ikx'} dx'}{\sum_{k=-\infty}^{\infty} e^{-\nu k^2 t + ikx} \int_0^{2\pi} e^{\cos x'/(2\nu)} e^{-ikx'} dx'}. \quad (\text{S67})$$

Note that the numerical oscillation is strong in the calculation of the SPE, so we only present the numerical solution at  $t \leq 1$ . The temporal evolution of the real and imaginary parts of  $\psi_{\pm}$  in Fig. S3(b-e) shows notable gradient magnitudes of the wave function at  $x = \pi$ , suggesting the shock formation.

- 
- [S1] Z. Meng and Y. Yang, Quantum computing of fluid dynamics using the hydrodynamic Schrödinger equation, Phys. Rev. Res. **5**, 033182 (2023).  
[S2] L. Salasnich, S. Succi, and A. Tiribocchi, Quantum wave representation of dissipative fluids (2023), arXiv:2308.05879.  
[S3] A. Chern, F. Knöppel, U. Pinkall, P. Schröder, and S. Weißmann, Schrödinger's smoke, ACM Trans. Graph. **35**, 1 (2016).  
[S4] A. Chern, F. Knöppel, U. Pinkall, and P. Schröder, Inside fluids: Clebsch maps for visualization and processing, ACM Trans. Graph. **36**, 1 (2017).

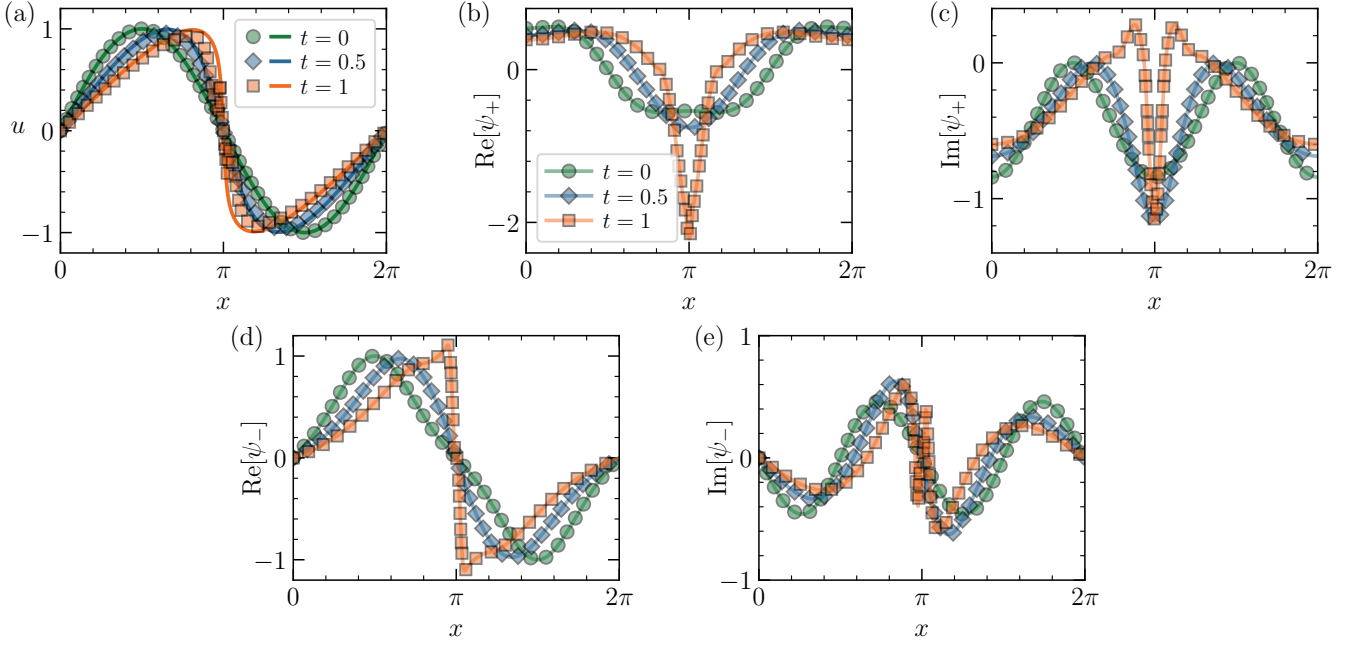


FIG. S3. Numerical results of the SPE equation equivalent to the Burgers equation. (a) Comparison of the reconstructed velocity (symbols) with the exact solution (lines). (b–e) Evolution of the real and imaginary parts of  $\psi_+$  and  $\psi_-$ .

- [S5] Z. Meng and Y. Yang, Lagrangian dynamics and regularity of the spin Euler equation (2023), arXiv:2311.05149.  
[S6] M. Suzuki, Fractal decomposition of exponential operators with applications to many-body theories and Monte Carlo simulations, *Phys. Lett. A* **146**, 319 (1990).  
[S7] M. Suzuki, General theory of fractal path integrals with applications to many-body theories and statistical physics, *J. Math. Phys.* **32**, 400 (1991).